Supplementary Material (ESI) for Organic & Biomolecular Chemistry

Electronic Supplementary Information

Simple 1-dicyanomethylene-2-chloro-3-aminoindene push-pull chromophores: applications in cation and anion sensing

Sara Basurto,[a] Daniel Miguel,[b] Daniel Moreno,[a] Ana G. Neo,[c] Roberto Quesada,[a] Tomás Torroba*[a]

[a] *Departamento de Química, Facultad de Ciencias, Universidad de Burgos, Plaza Misael Bañuelos s/n, 09001 Burgos, Spain. Fax: 34 947 258831; Tel: 34 947 258088; E-mail: ttorroba@ubu.es*
[b] *Departamento de Química Física y Química Inorgánica, Facultad de Ciencias, Universidad de Valladolid, 47011 Valladolid, Spain. Fax: 34 983 423234; Tel: 34 983 184096; E-mail: dmsj@qi.uva.es*
[c] *Departamento de Química Orgánica, Facultad de Veterinaria, Universidad de Extremadura, Avenida de la Universidad s/n, 10071 Cáceres, Spain. Fax: 34 927 257110; Tel: 34 927 257158; E-mail: aneo@unex.es*

Contents:

1. Crystal Structure determination for compound 3 A single crystal of **3** was mounted on a glass fibre. X-ray measurements were made using a Bruker SMART CCD area-detector diffractometer with Mo-K_α radiation (λ = 0.71073 Å).[1a] Intensities were integrated[1b] from several series of exposures, each exposure covering 0.3° in ω, and the total data set being a sphere. Absorption corrections were applied, based on multiple and symmetry-equivalent measurements.[1c] The structure was solved by direct methods and refined by least squares on weighted F^2 values for all reflections.[1d] All non-hydrogen atoms were assigned anisotropic displacement parameters and refined without positional constraints. All hydrogen atoms were constrained to ideal geometries and refined with fixed isotropic displacement parameters. Refinement proceeded smoothly to give the residuals. Complex neutral-atom scattering factors were used.[1e]

Table 1. Crystal data and structure refinement for **3**.

Identification code	neo163am	
Empirical formula	C20 H22 Cl N3	
Formula weight	339.86	
Temperature	293(2) K	
Wavelength	0.71073 Å	
Crystal system	Triclinic	
Space group	P-1	
Unit cell dimensions	a = 8.3304(16) Å	α= 92.955(4)°.
	b = 9.1897(18) Å	β= 97.382(4)°.
	c = 13.096(3) Å	γ = 108.536(4)°.
Volume	938.1(3) $Å^3$	
Z	2	
Density (calculated)	1.203 Mg/m^3	
Absorption coefficient	0.209 mm^{-1}	
F(000)	360	
Crystal size	0.31 x 0.13 x 0.09 mm^3	
Theta range for data collection	1.58 to 23.33°.	
Index ranges	-9<=h<=9, -10<=k<=8, -14<=l<=12	
Reflections collected	4227	
Independent reflections	2673 [R(int) = 0.0248]	
Completeness to theta = 23.33°	98.3 %	
Absorption correction	Semi-empirical from equivalents	
Max. and min. transmission	1.000000 and 0.627933	

Refinement method	Full-matrix least-squares on F^2
Data / restraints / parameters	2673 / 0 / 221
Goodness-of-fit on F^2	1.038
Final R indices [I>2sigma(I)]	R1 = 0.0635, wR2 = 0.1733
R indices (all data)	R1 = 0.0874, wR2 = 0.1891
Largest diff. peak and hole	0.477 and -0.403 e.Å^{-3}

1 (a) *SMART diffractometer control software*, Bruker Analytical X-ray Instruments Inc., Madison, WI, 2000. (b) *SAINT integration software*, Siemens Analytical X-ray Instruments Inc., Madison, WI, 2000. (c) G. M. Sheldrick, *SADABS: A program for absorption correction with the Siemens SMART system*; University of Göttingen: Germany, 2001. (d) *SHELXTL program system version 6.1*; Bruker Analytical X-ray Instruments Inc., Madison, WI, 1998. (e) *International Tables for Crystallography*, Kluwer, Dordrecht, 1992, vol. C.

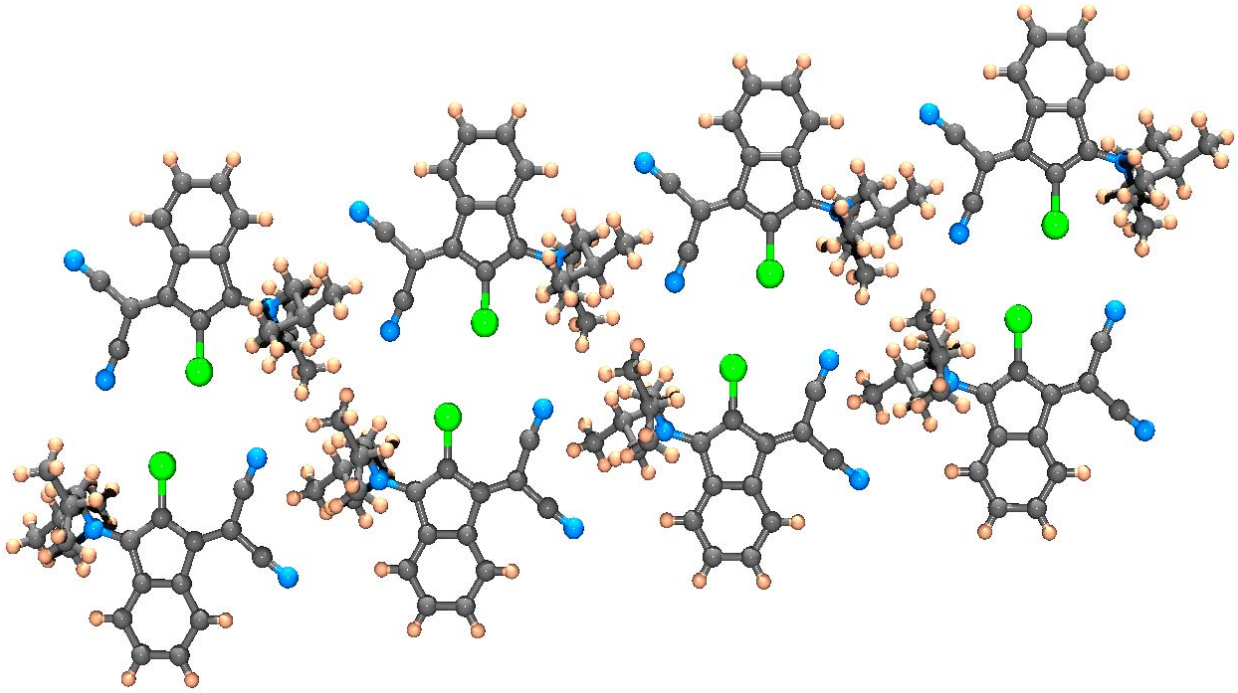

Fig. 1. Crystal packing of **3**

2. NMR and UV spectra of compounds 2-10.

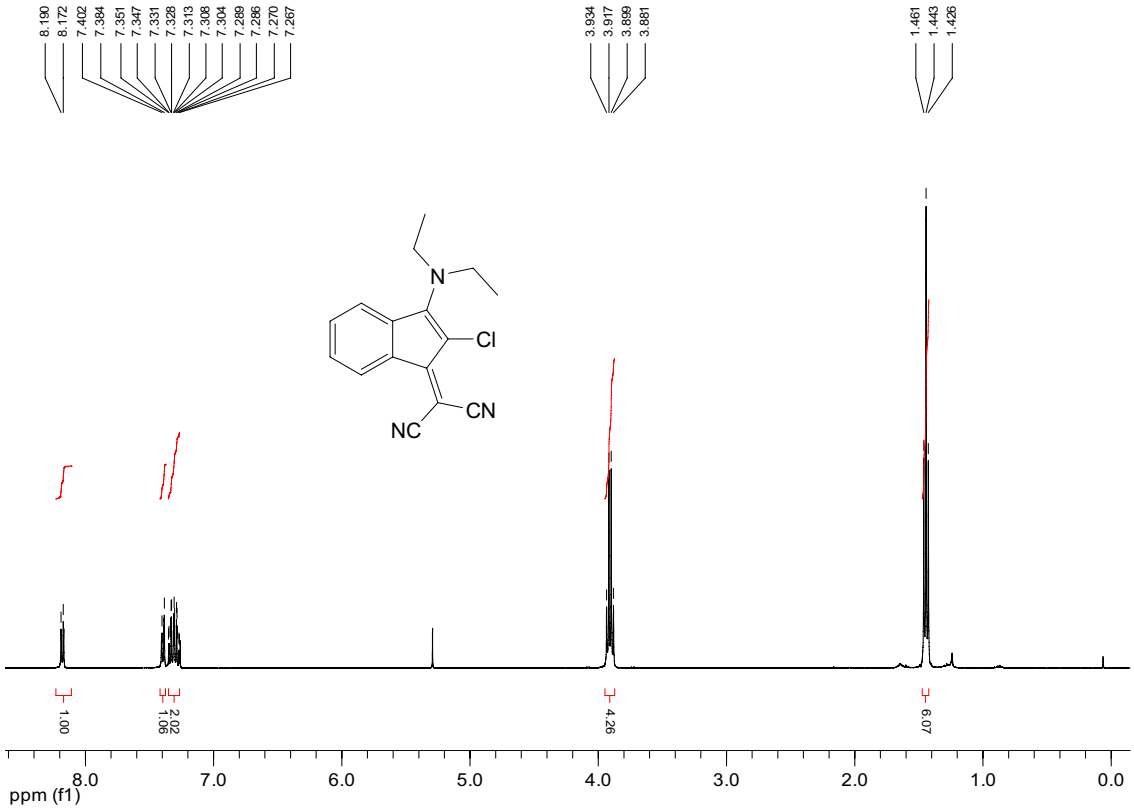

Fig. 2. ^{1}H NMR ($CDCl_3$, 400 MHz) of **2**

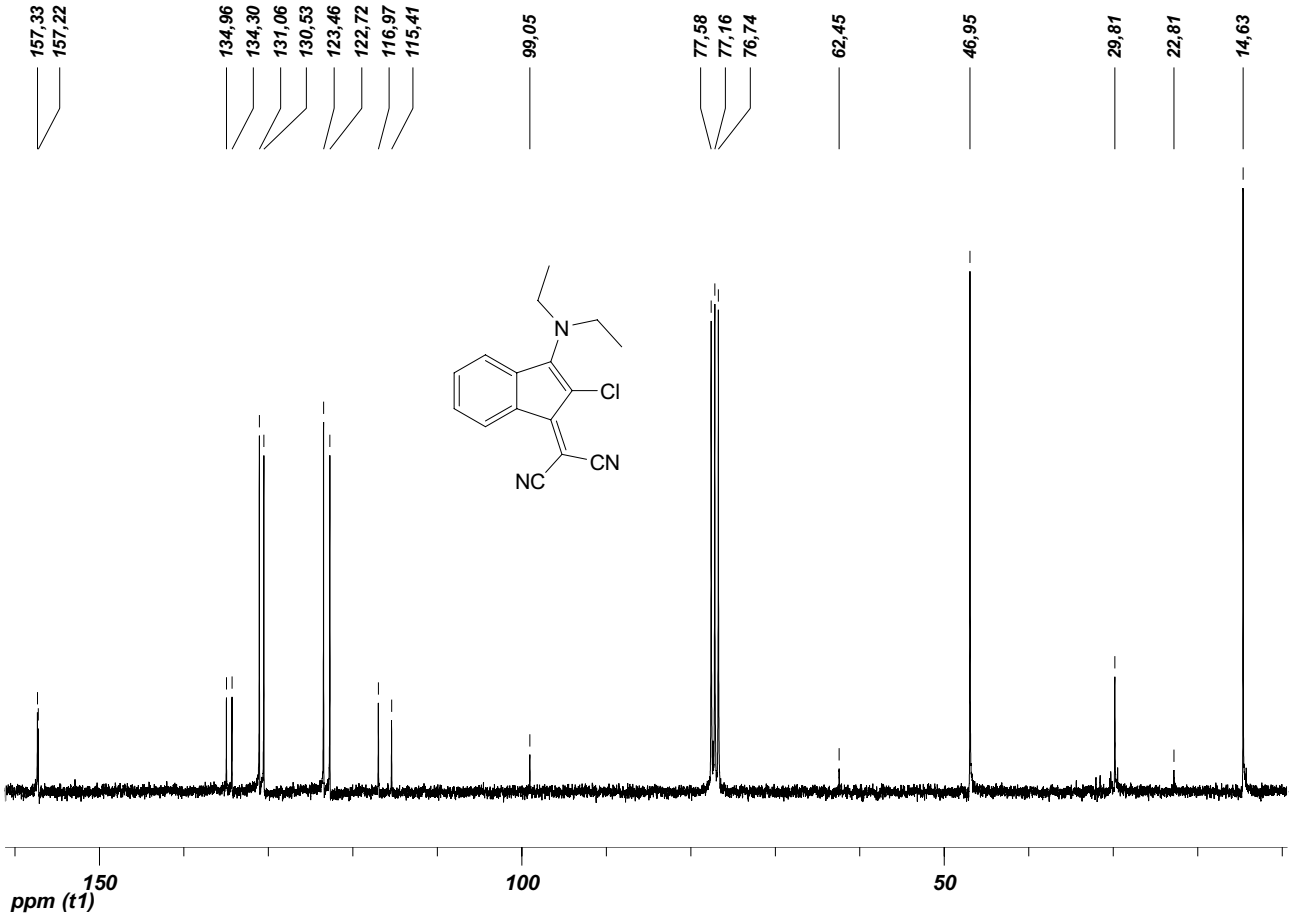

Fig. 3. ^{13}C NMR ($CDCl_3$, 75 MHz) of **2**

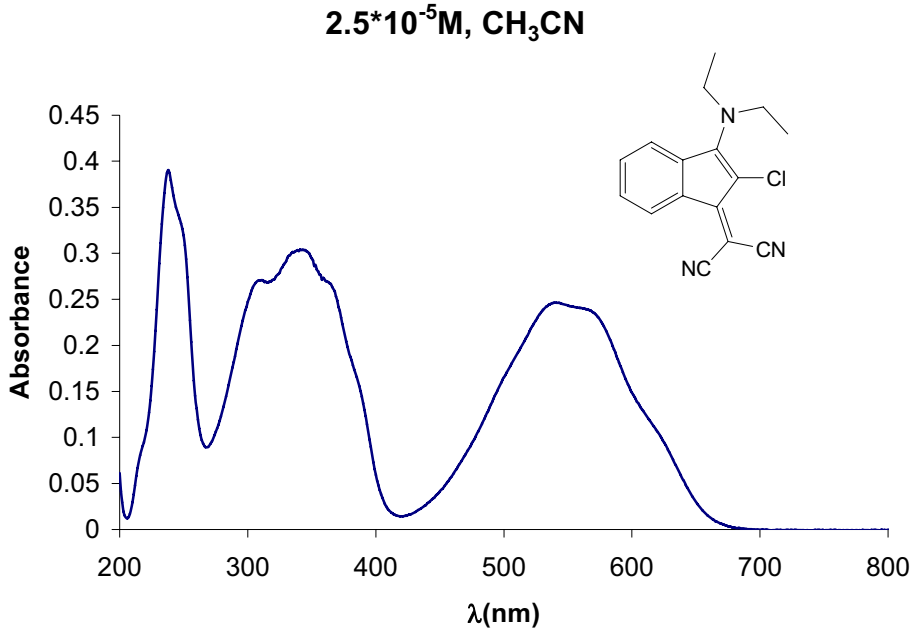

Fig. 4. UV-vis (CH_3CN, 2.5x10^{-5} M) of **2**

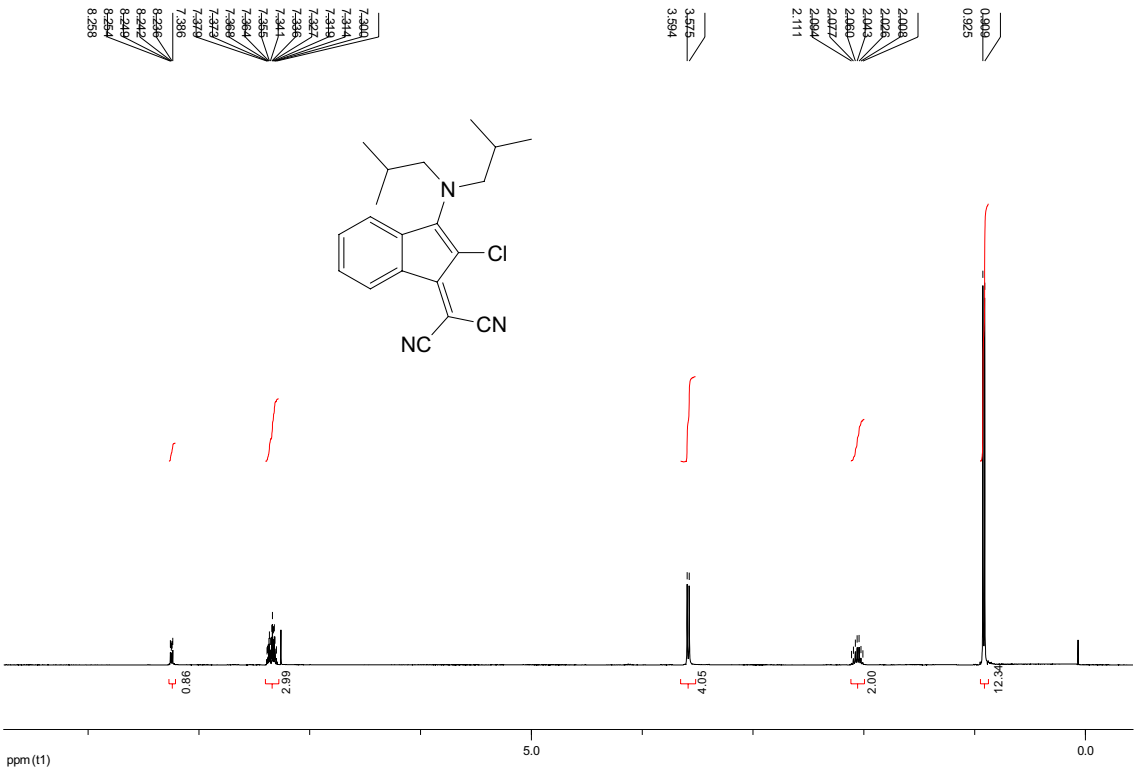

Fig. 5. ^{1}**H NMR** ($CDCl_3$, 400 MHz) of **3**

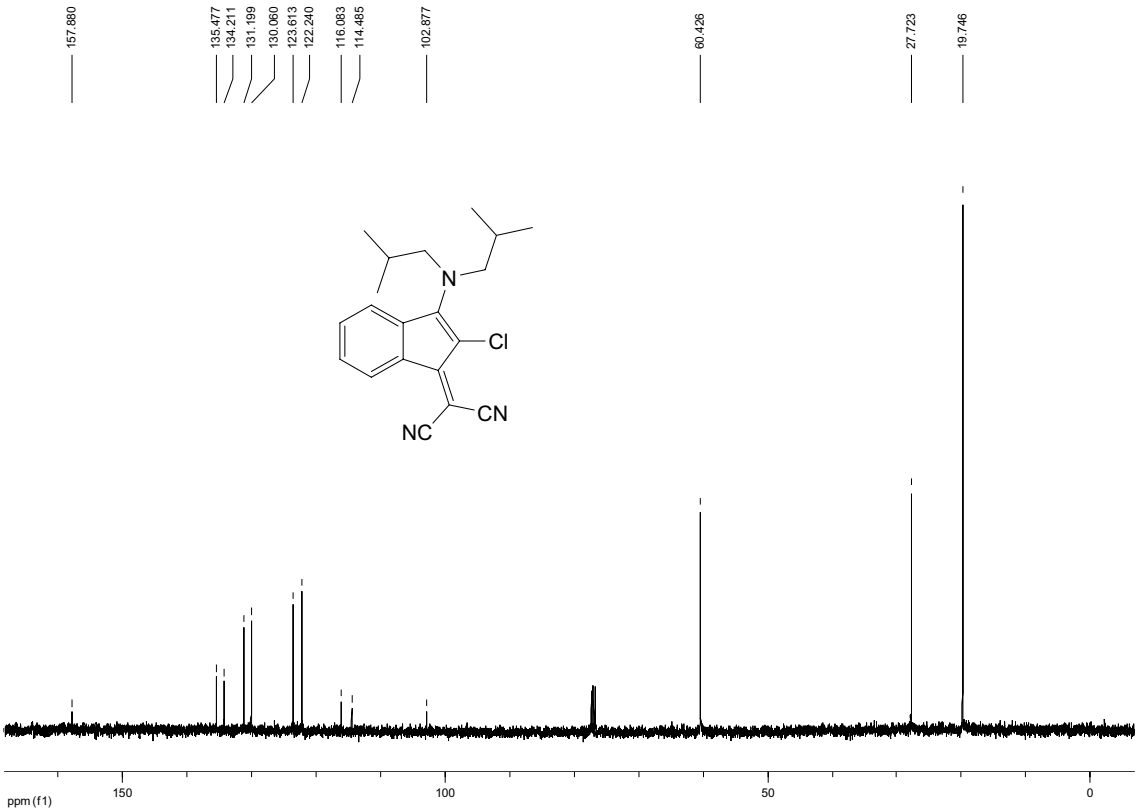

Fig. 6. ^{13}**C NMR** ($CDCl_3$, 100 MHz) of **3**

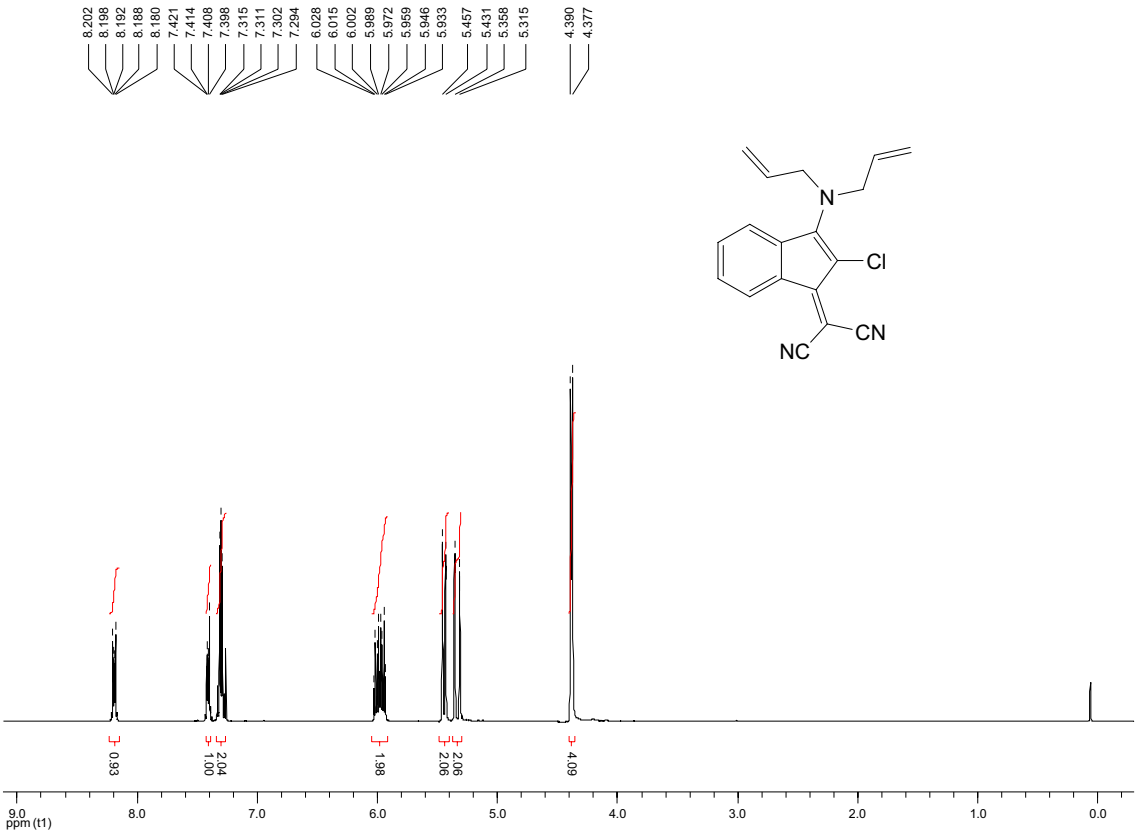

Fig. 7. ^{1}**H NMR** ($CDCl_3$, 400 MHz) of **4**

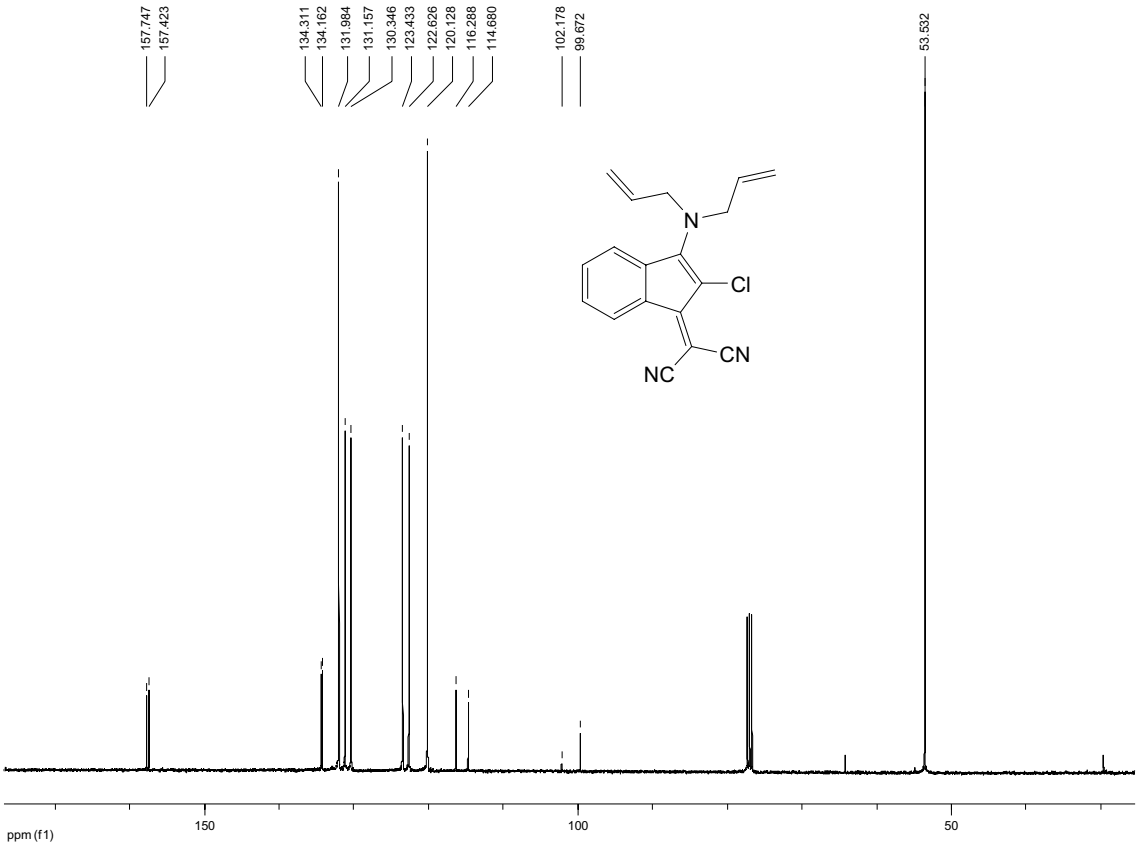

Fig. 8. ^{13}**C NMR** ($CDCl_3$, 100 MHz) of **4**

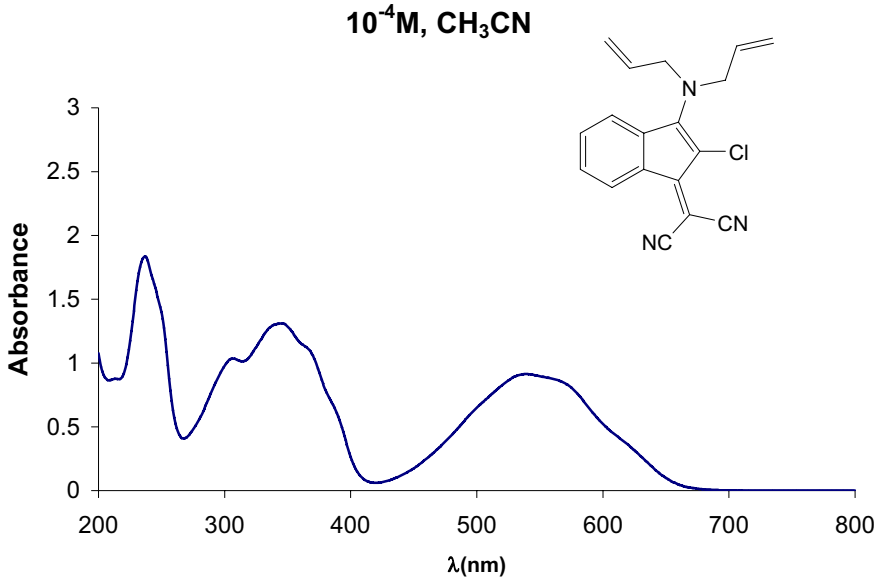

Fig. 9. UV-vis (CH_3CN, 10^{-4} M) of **4**

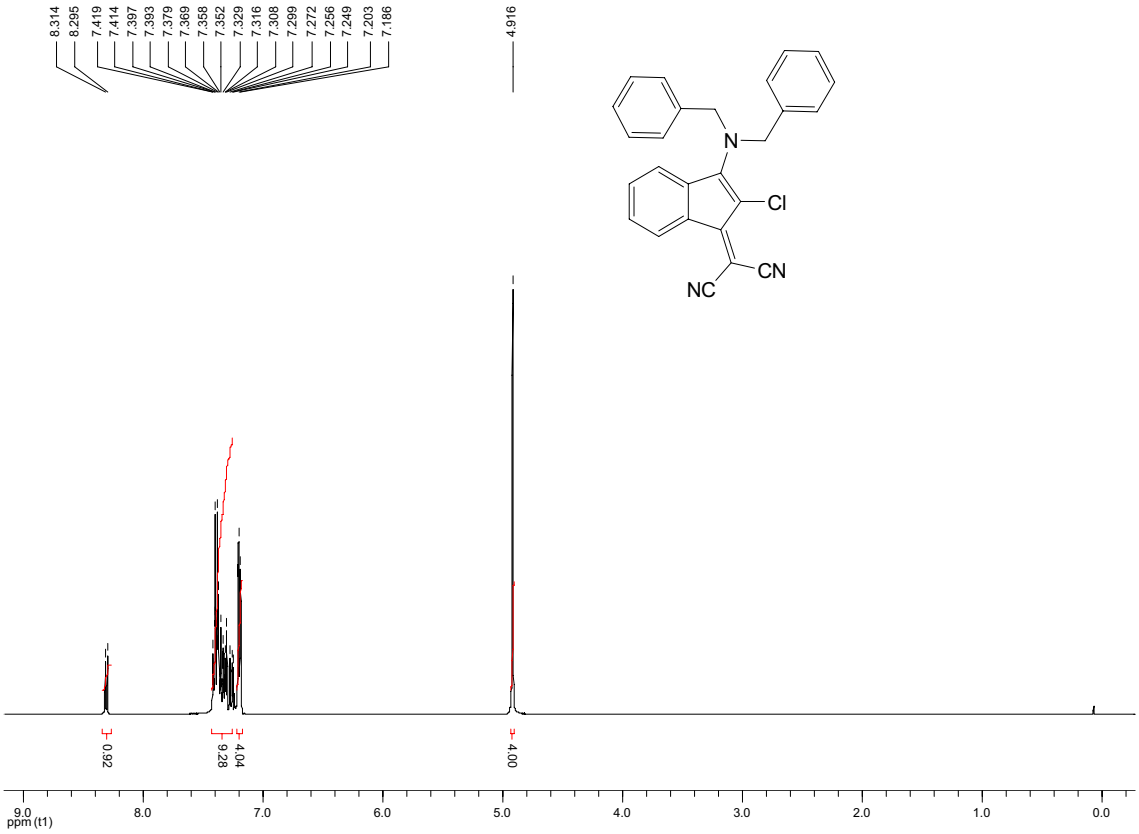

Fig. 10. ^{1}H NMR ($CDCl_3$, 400 MHz) of **5**

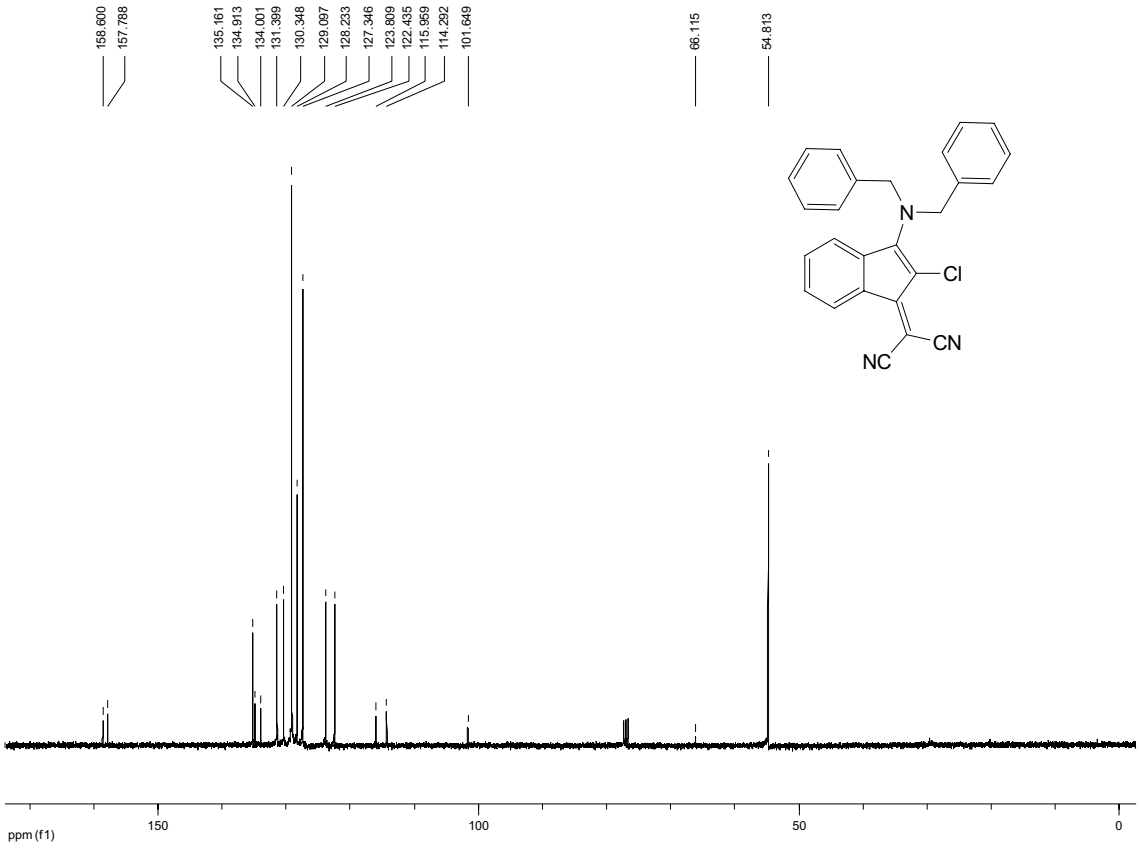

Fig. 11. ^{13}**C NMR** ($CDCl_3$, 100 MHz) of **5**

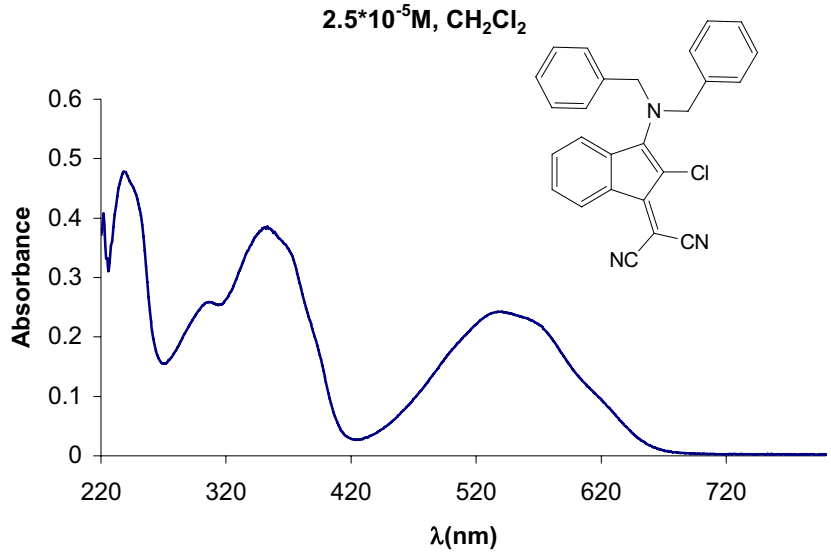

Fig. 12. UV-vis (CH_2Cl_2, 2.5x10^{-5} M) of **5**

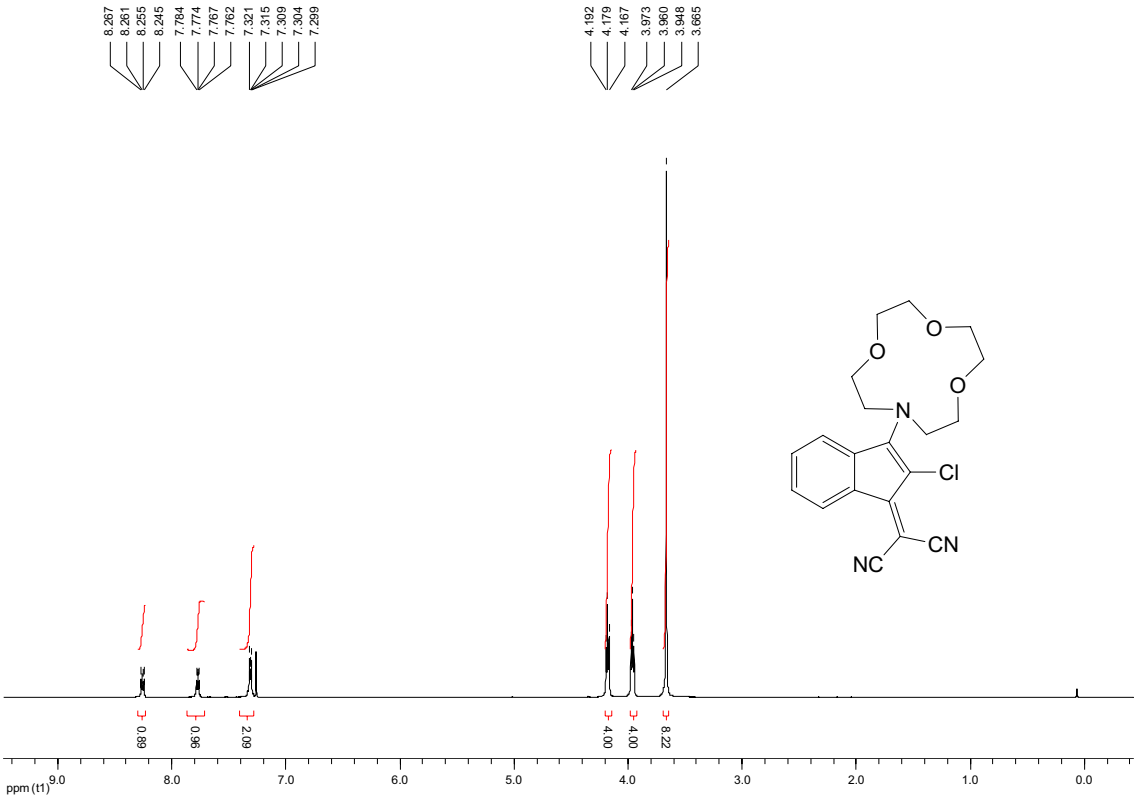

Fig. 13. ^{1}**H NMR** ($CDCl_3$, 400 MHz) of **6**

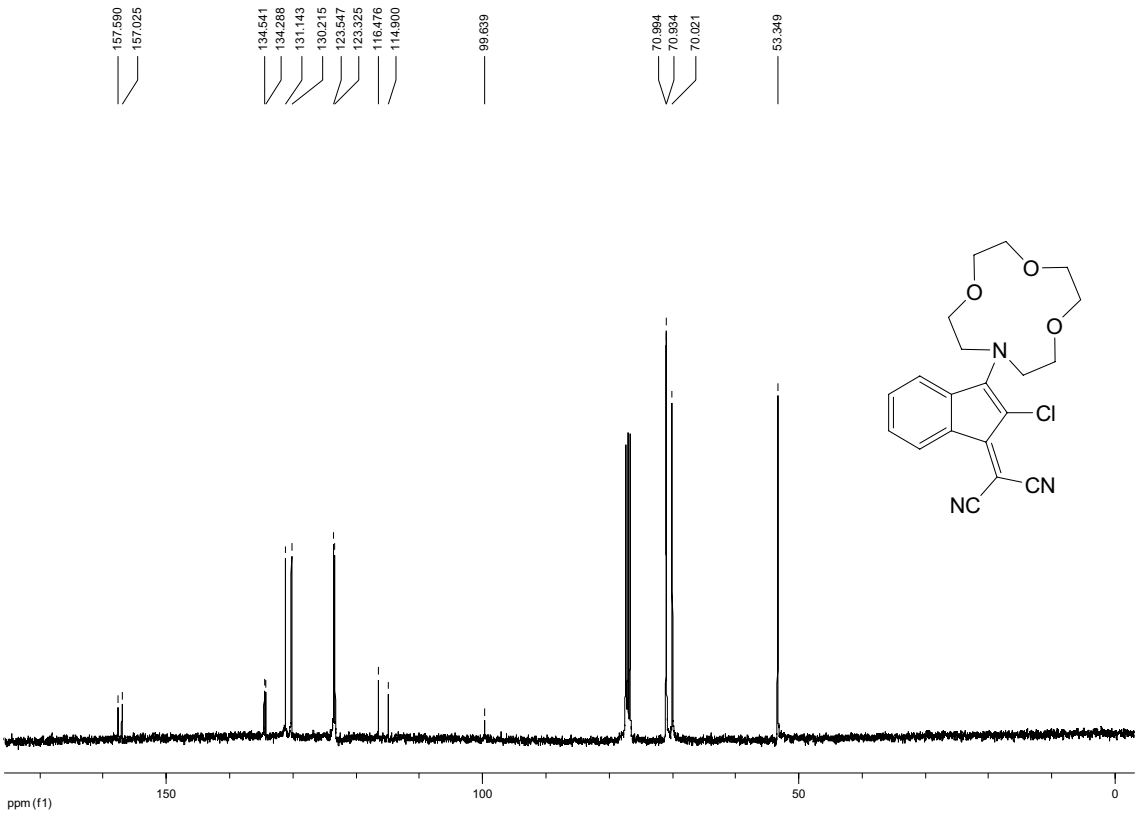

Fig. 14. ^{13}**C NMR** ($CDCl_3$, 100 MHz) of **6**

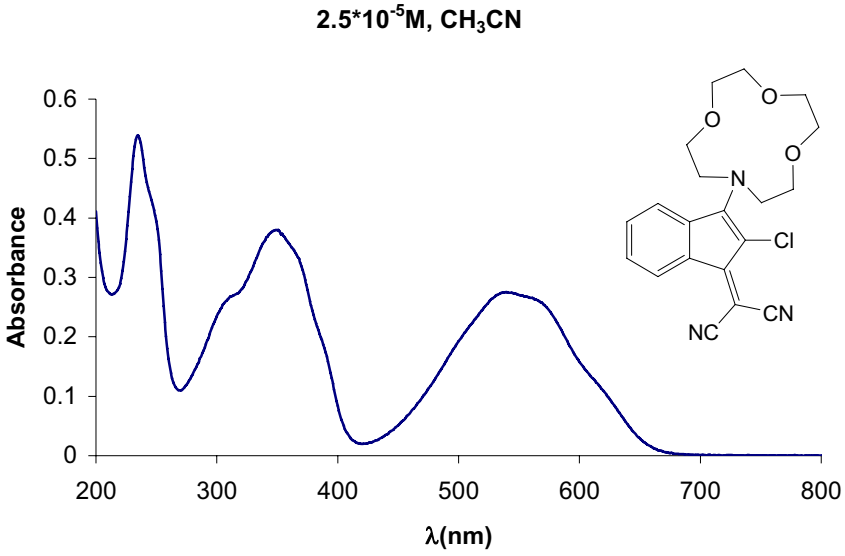

Fig. 15. UV-vis (CH_2Cl_2, 2.5x10^{-5} M) of **6**

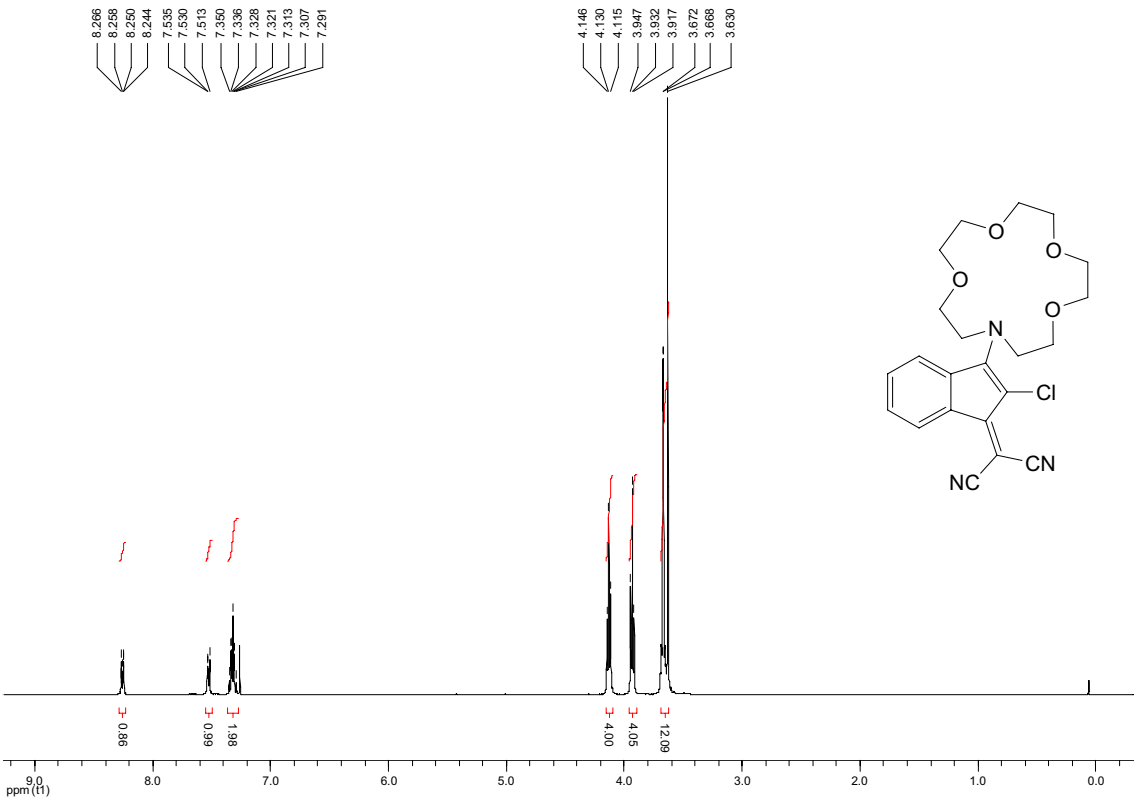

Fig. 16. ^{1}H NMR ($CDCl_3$, 400 MHz) of **7**

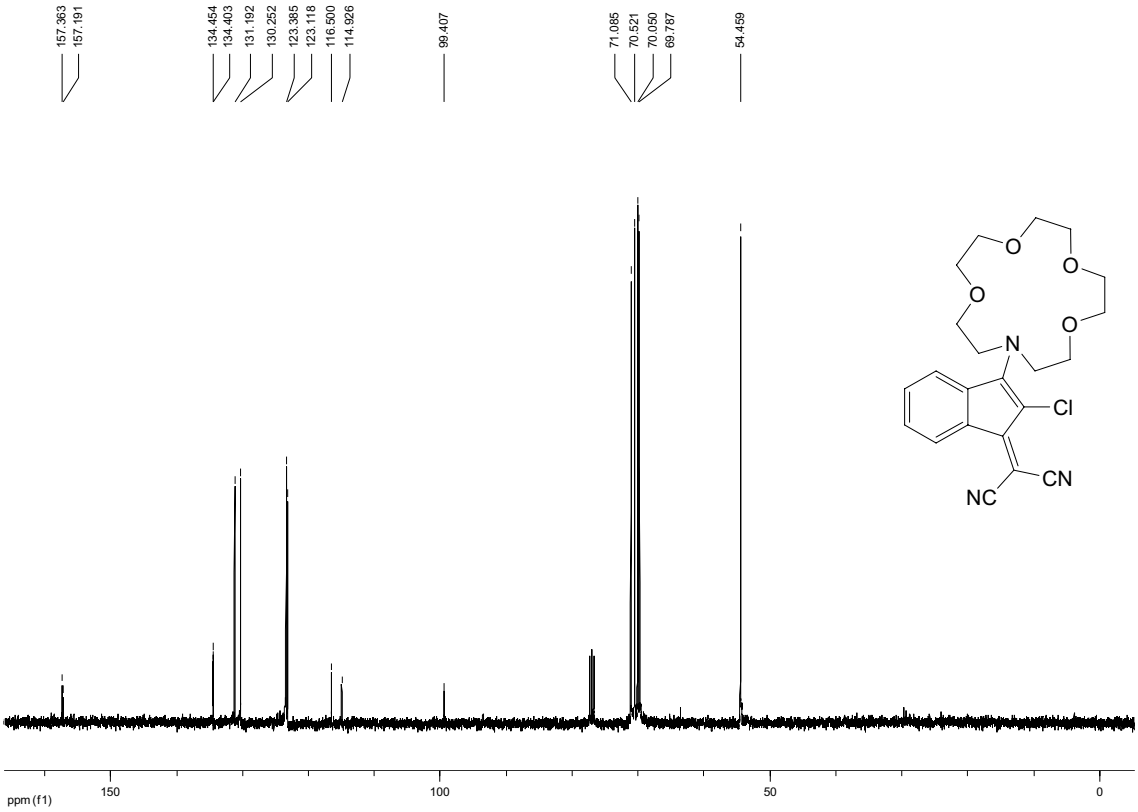

Fig. 17. ^{13}**C NMR** ($CDCl_3$, 100 MHz) of **7**

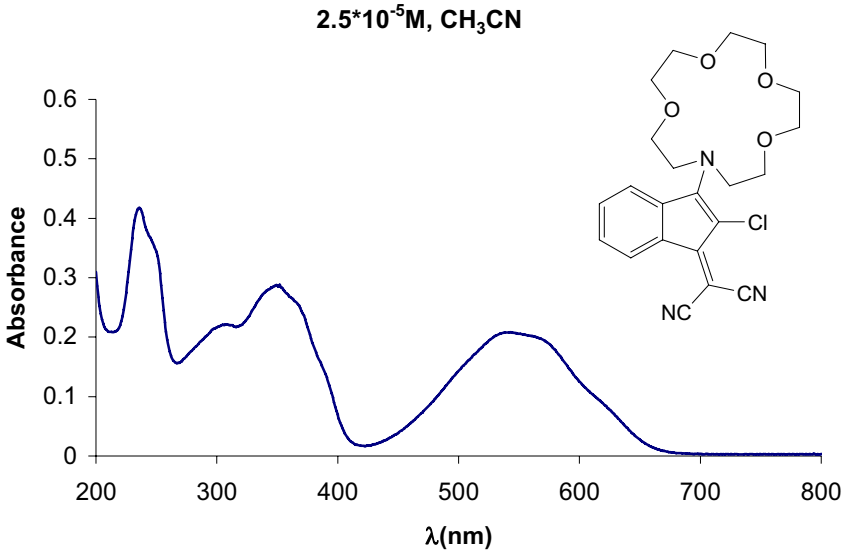

Fig. 18. UV-vis (CH_2Cl_2, 2.5x10^{-5} M) of **7**

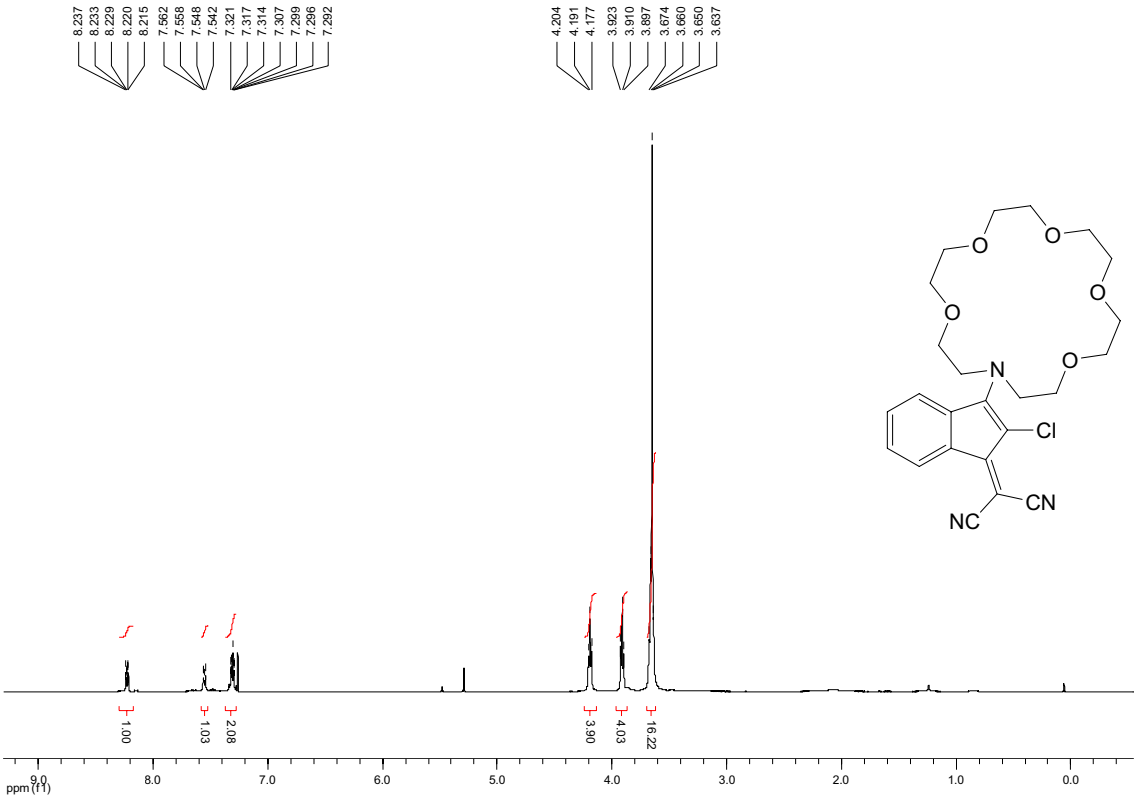

Fig. 19. ^{1}H NMR ($CDCl_3$, 400 MHz) of **8**

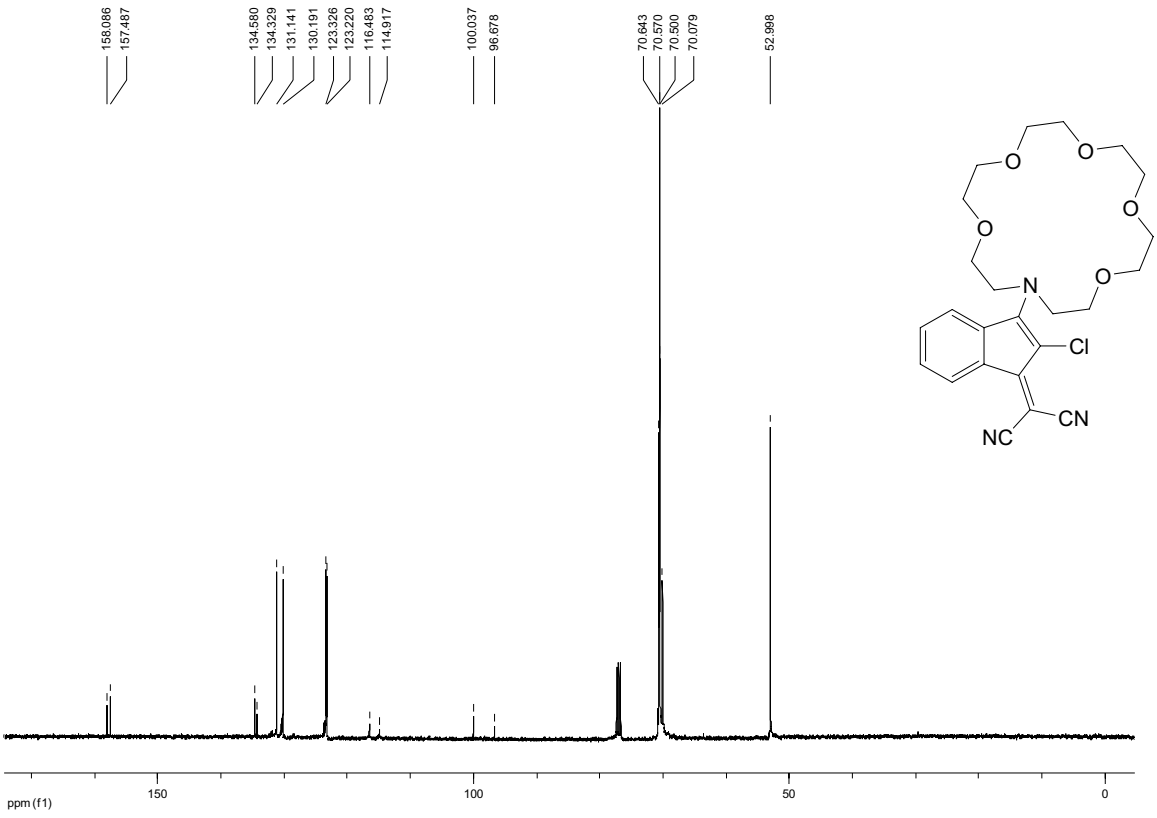

Fig. 20. ^{13}C NMR ($CDCl_3$, 100 MHz) of **8**

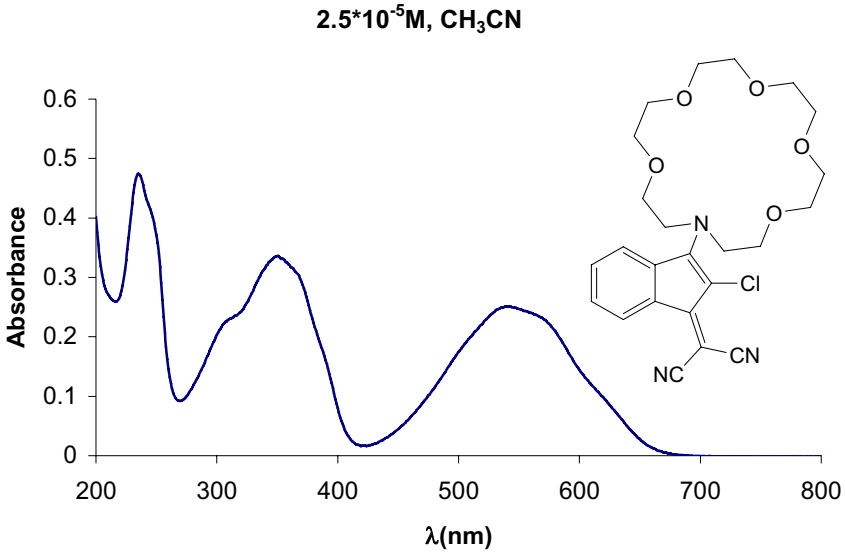

Fig. 21. UV-vis (CH_2Cl_2, 2.5x10^{-5} M) of **8**

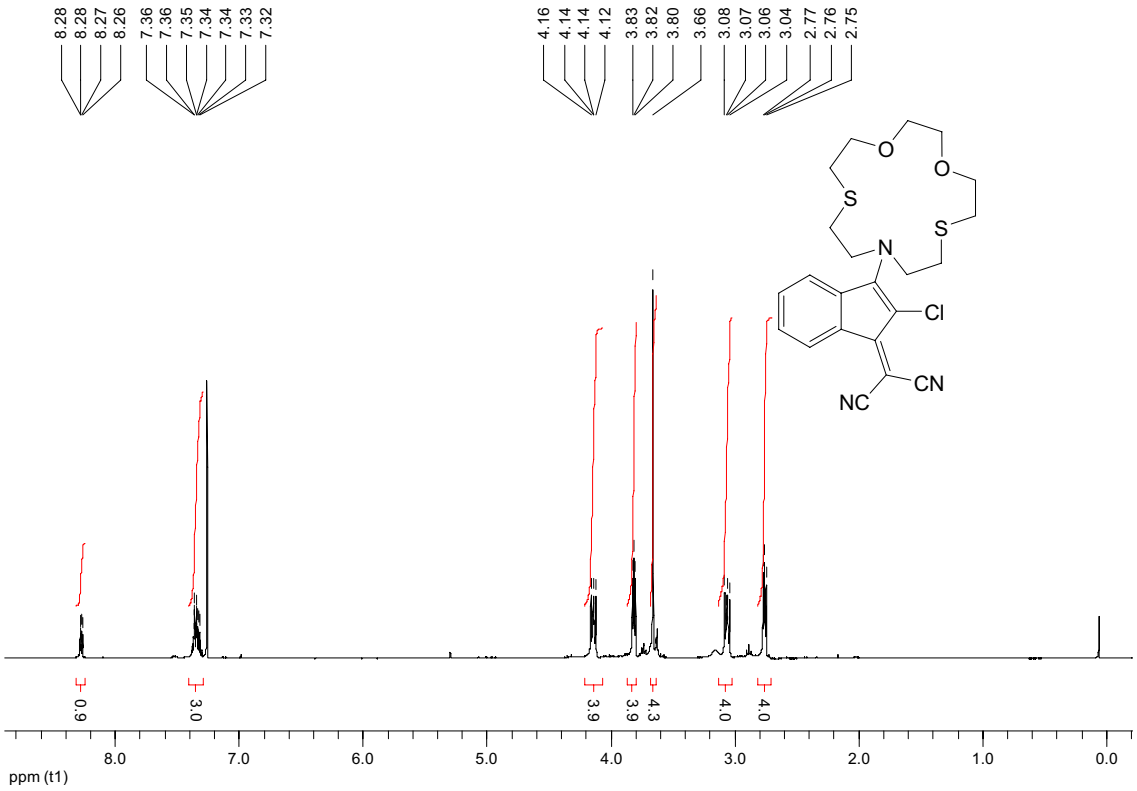

Fig. 22. ^{1}H NMR ($CDCl_3$, 400 MHz) of **9**

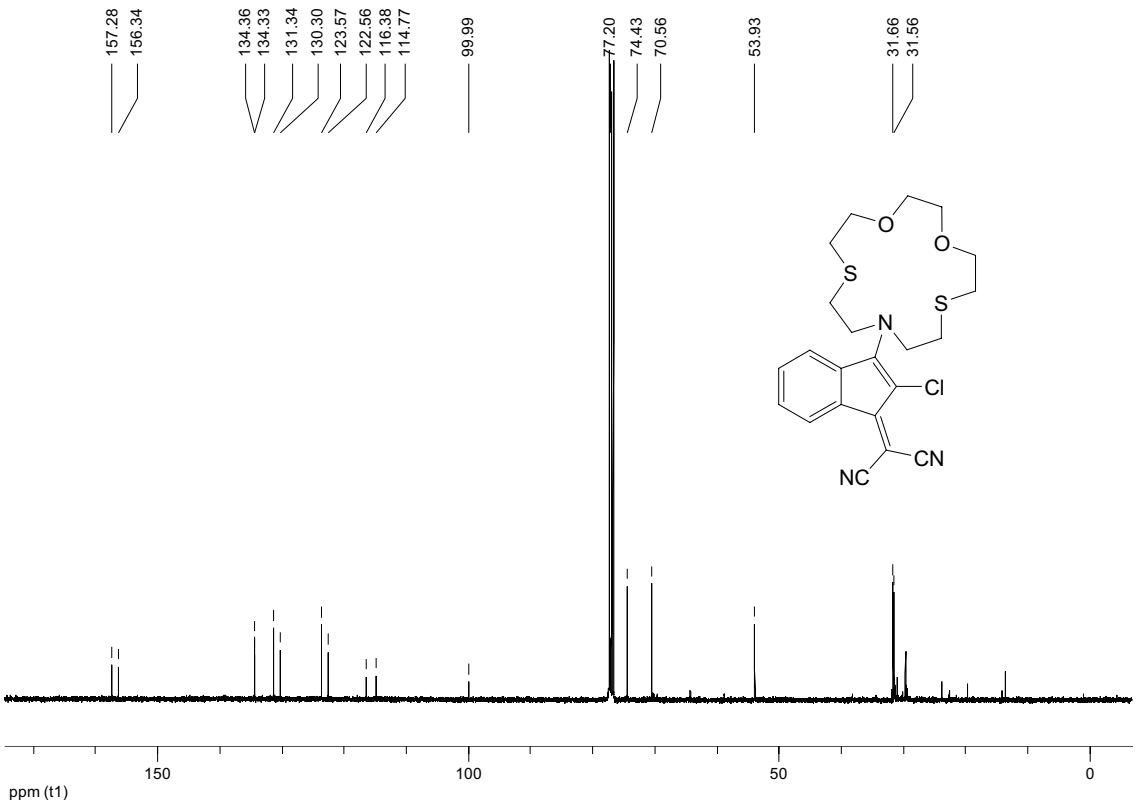

Fig. 23. ^{13}**C NMR** ($CDCl_3$, 100 MHz) of **9**

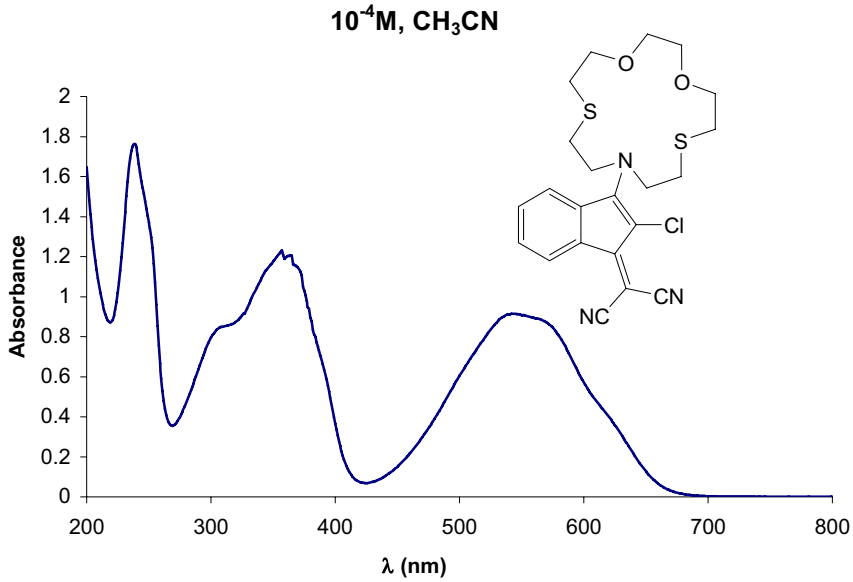

Fig. 24. UV-vis (CH_3CN, 10^{-4} M) of **9**

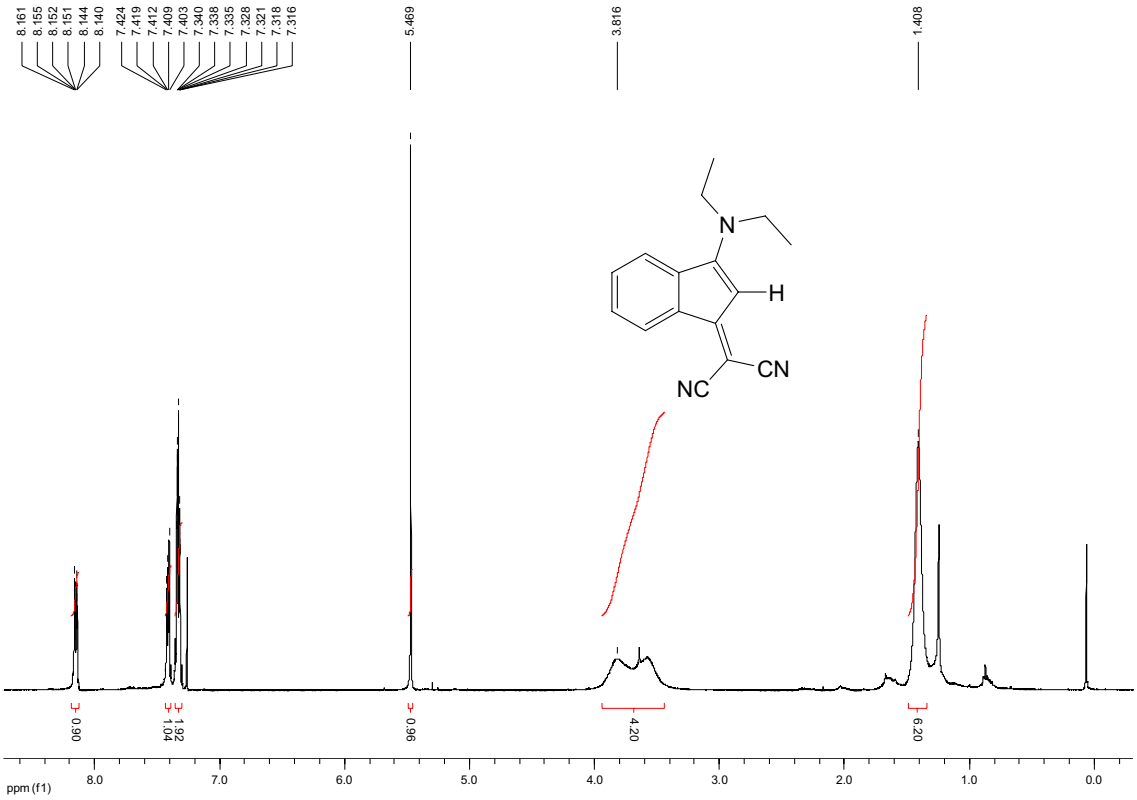

Fig. 25. ^{1}**H NMR** ($CDCl_3$, 400 MHz) of **10**

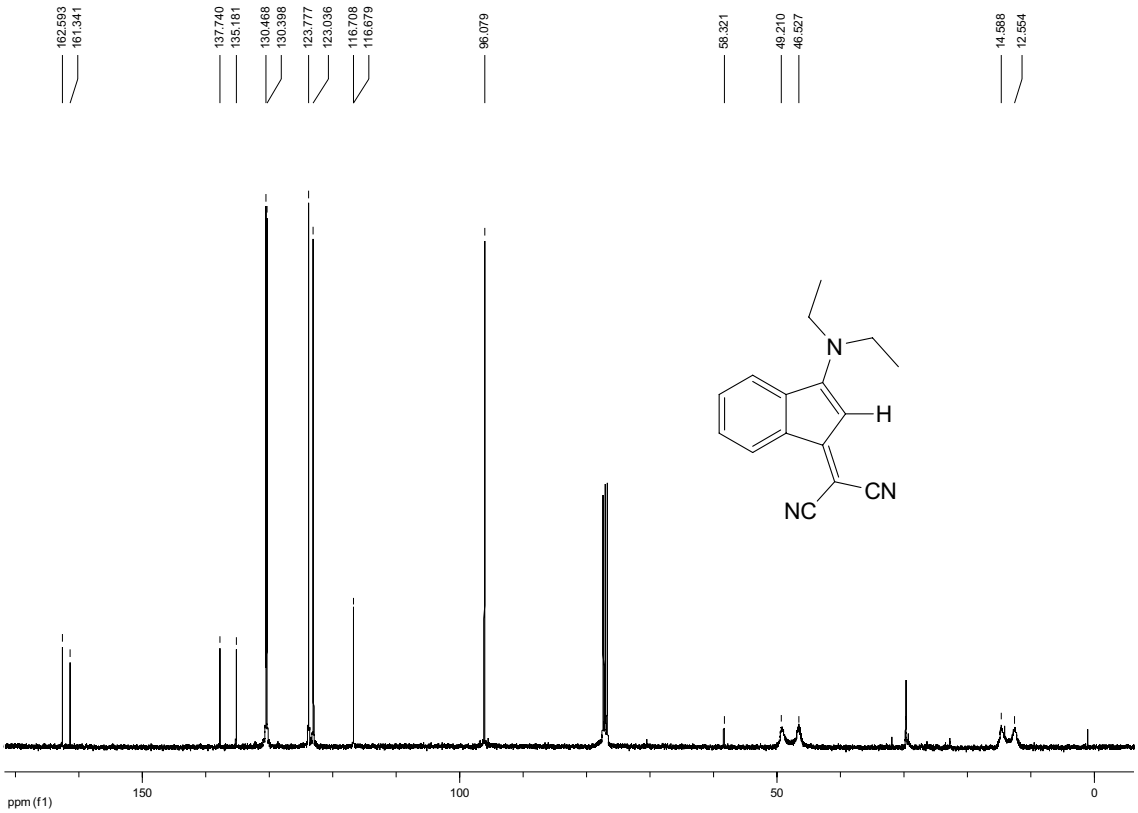

Fig. 26. ^{13}**C NMR** ($CDCl_3$, 100 MHz) of **10**

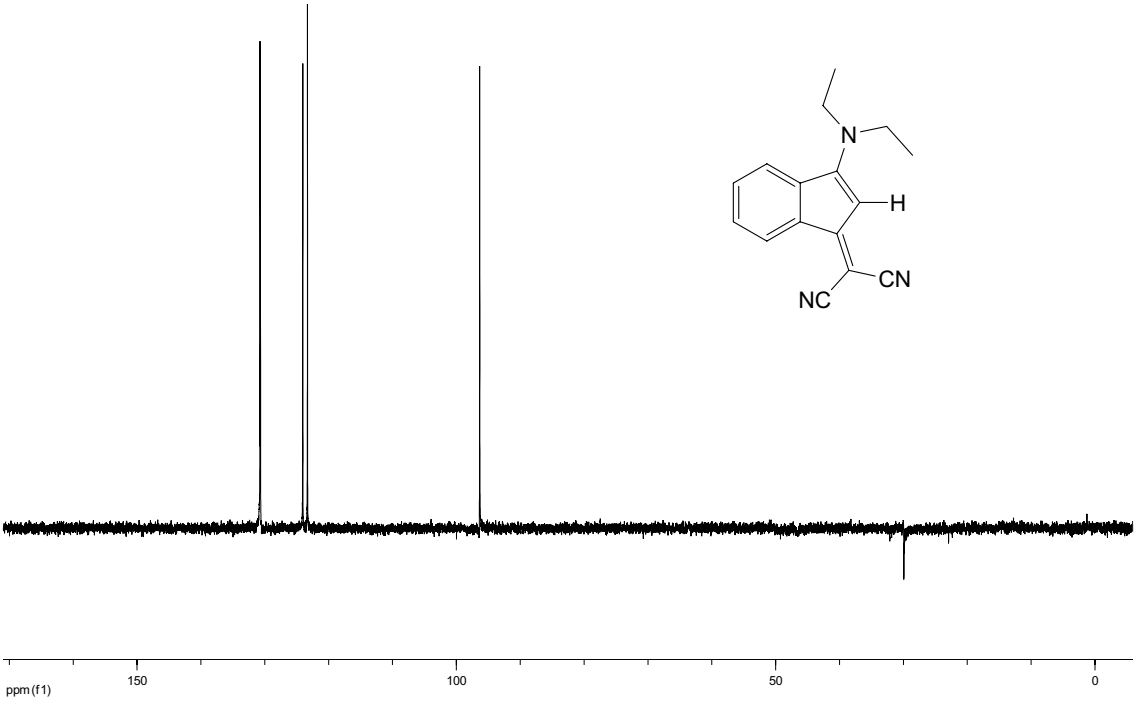

Fig. 27. DEPT NMR ($CDCl_3$, 100 MHz) of **10**

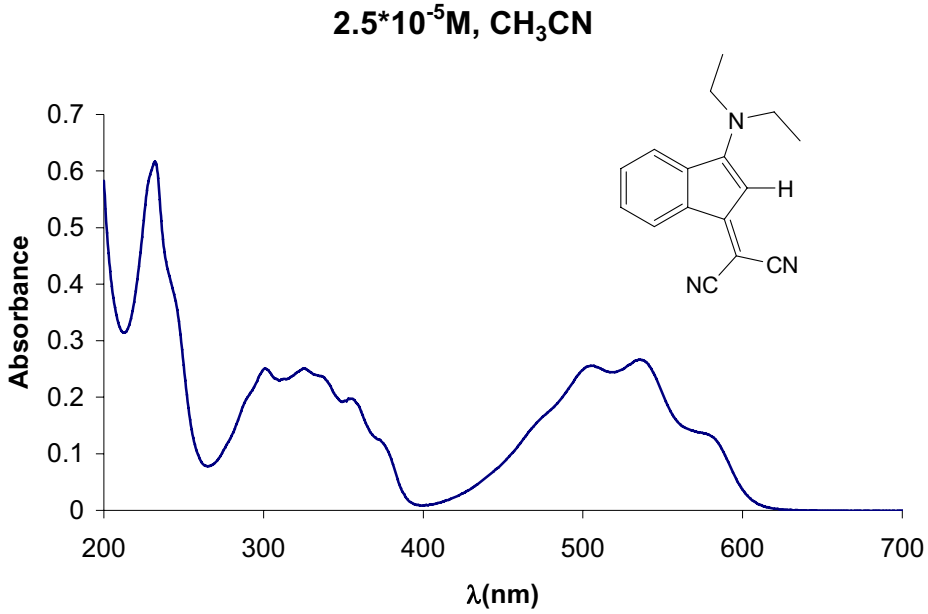

Fig. 28. UV-vis (CH_3CN, 2.5x10^{-5} M) of **10**

3. Titration Materials and Methods.

Perchlorate salts were used for some cations and triflate salts for the rest of cations:

CATION	*SALT*
Ag^{+}	$AgClO_4 \cdot xH_2O$
Ni^{2+}	$Ni(ClO_4)_2 \cdot 6H_2O$
Sn^{2+}	$Sn(CF_3SO_3)_2$
Cd^{2+}	$Cd(ClO_4)_2$
Zn^{2+}	$Zn(CF_3SO_3)_2$
Pb^{2+}	$Pb(ClO_4)_2$
Cu^{2+}	$Cu(ClO_4)_2 \cdot 6H_2O$
Fe^{3+}	$Fe(ClO_4)_3 \cdot xH_2O$
Sc^{3+}	$Sc(CF_3SO_3)_3$
Al^{3+}	$Al(ClO_4)_3 \cdot 9H_2O$
Hg^{2+}	$Hg(ClO_4)_2$

5×10^{-2} M, 5×10^{-3} M, 5×10^{-4} M solutions of every salt were prepared, then a 10^{-4} M solution of the compound under study was prepared. For qualitative experiments, 2 mL solution of the compound under study were measured and the corresponding amount of salt was added by micropipette.

Eppendorf Research micropipette characteristics:

MODEL	Ep T.I.P.S.	Volume	Systematic error of measurement	Random error of measurement (CV)
2 - 20µL	2 - 200	2 µL	± 5.0 %	≤ 1.5 %
		10 µL	± 1.2 %	≤ 0.6 %
		20 µL	± 1.0 %	≤ 0.3 %
10 - 100µL	2 - 200	10 µL	± 3.0 %	≤ 1.0 %
		50 µL	± 1.0 %	≤ 0.3 %
		100 L	± 0.8 %	≤ 0.2 %
100 - 1000µL	50 - 1000	100 µL	± 3.0 %	≤ 0.6 %
		5000 µL	± 1.0 %	≤ 0.2 %
		1000 µL	± 0.6 %	≤ 0.2 %
500 - 5000µL	100 - 5000	500 µL	± 2.4 %	≤ 0.6 %
		2500 µL	± 1.2 %	≤ 0.25 %
		5000 µL	± 0.6 %	≤ 0.15 %

4. Colorimetric studies

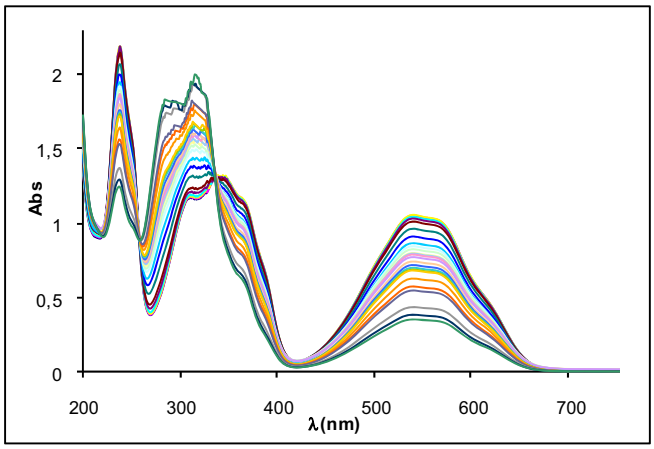

Fig. 29. UV titration of **2** (10^{-4} M, CH_3CN) with Sc^{3+}

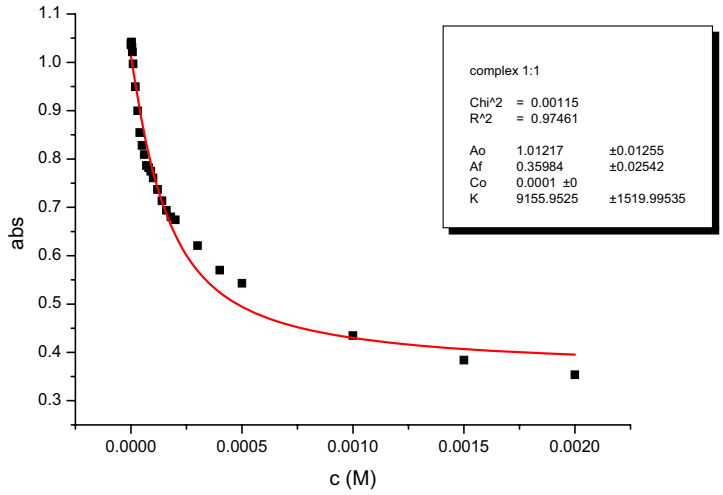

Fig. 30. Titration profile of **2** (10^{-4} M, CH_3CN) and Sc^{3+}, λ=550nm

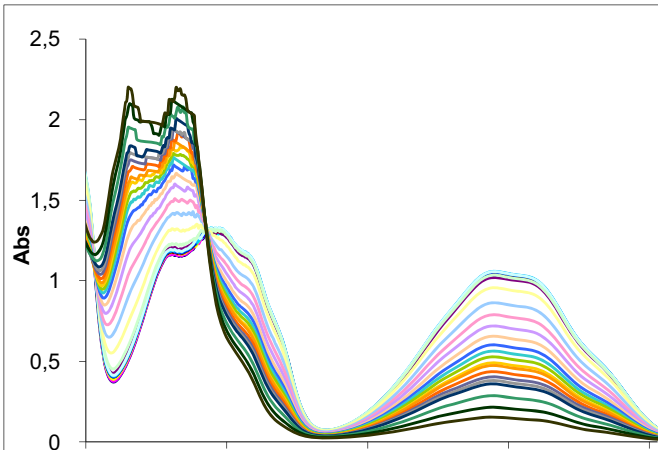

Fig. 31. UV titration of **2** (10^{-4} M, CH_3CN) with Sn^{2+}

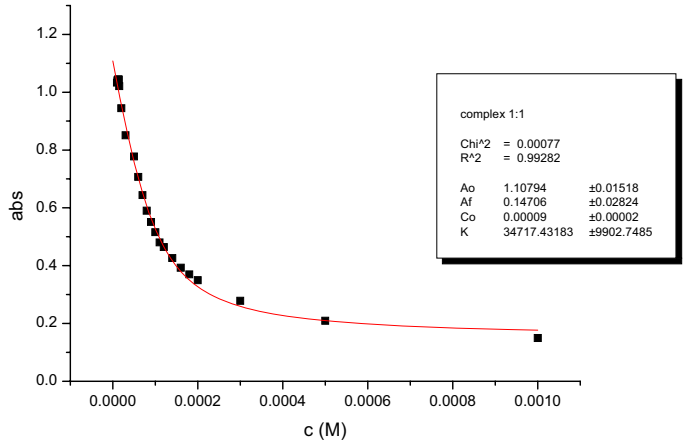

Fig. 32. Titration profile of **2** (10^{-4} M, CH_3CN), with Sn^{2+}, λ=550nm

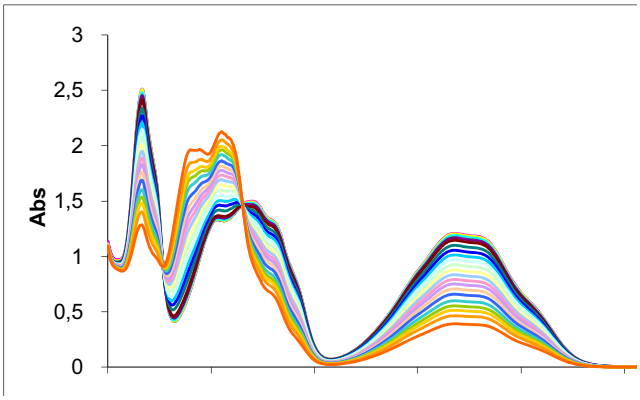

Fig. 33. UV titration of **2** (10^{-4} M, CH_3CN), with Al^{3+}.

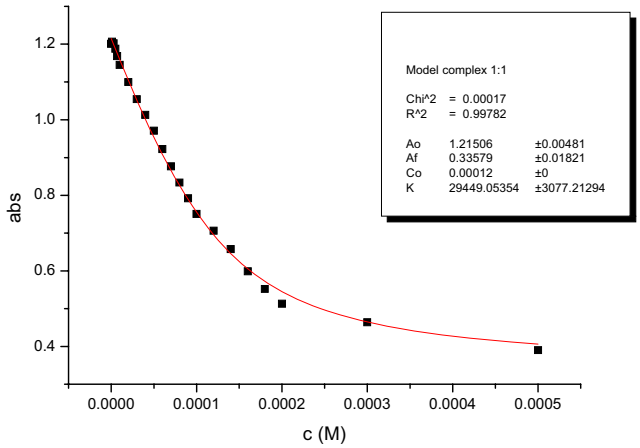

Fig. 34. Titration profile of **2** (10^{-4} M, CH_3CN), and Al^{3+} λ=550nm

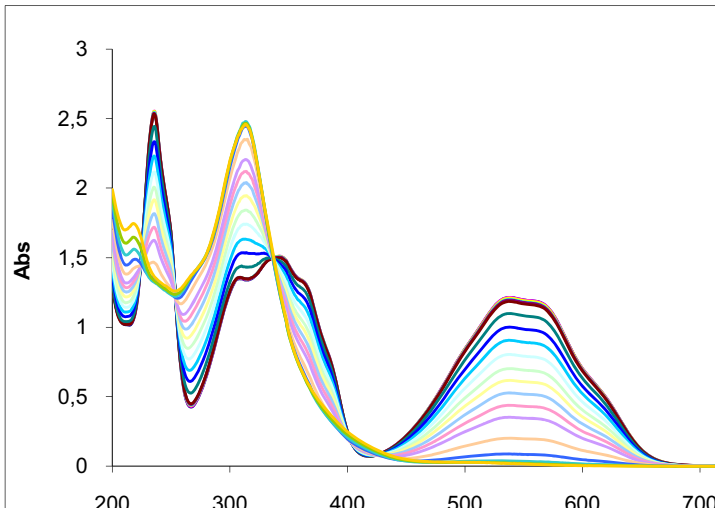

Fig. 35. UV titration of **2** (10^{-4} M, CH_3CN) with Fe^{3+}.

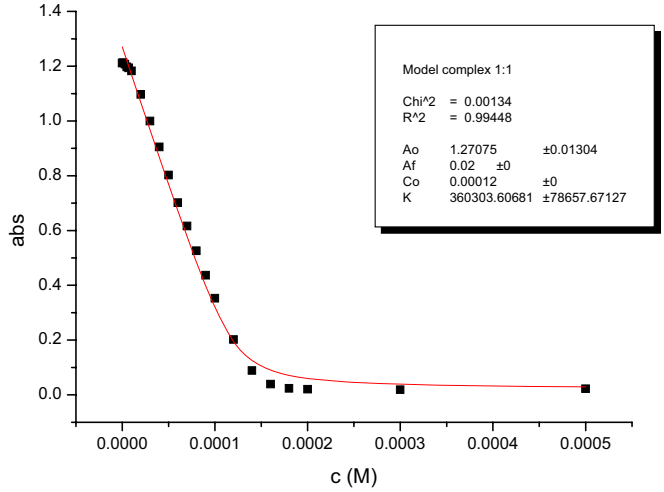

Fig. 36. Titration profile of **2** (10^{-4} M, CH_3CN) with Fe^{3+} λ=550nm

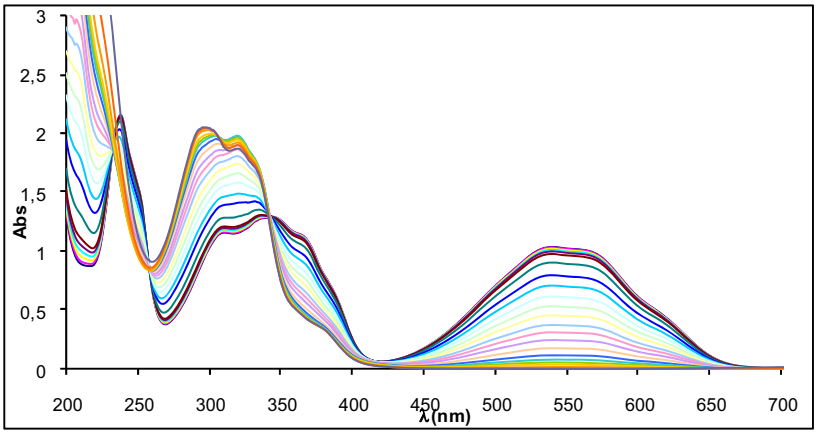

Fig. 37. UV titration of **2** (10^{-4} M, CH_3CN) with Cu^{2+}

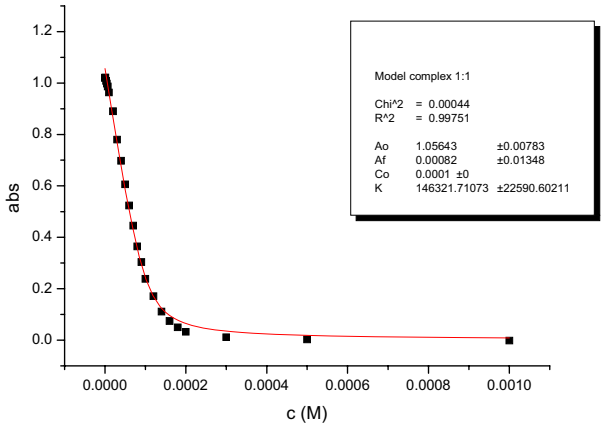

Fig. 38. Titration profile of **2** (10^{-4} M, CH_3CN) with Cu^{2+}

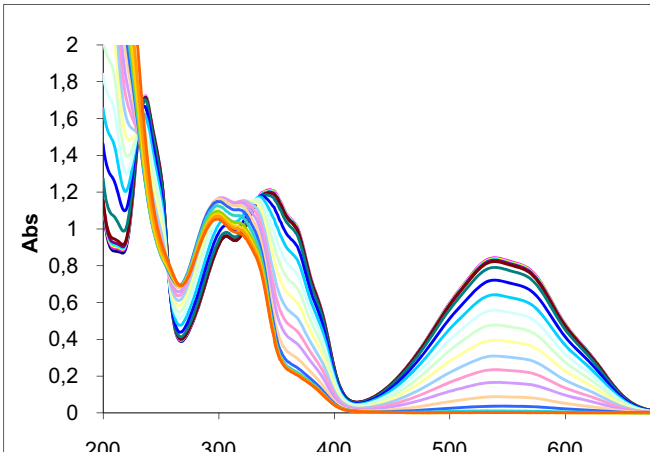

Fig. 39. UV titration of **4** (10^{-4} M, CH_3CN) with Cu^{2+}

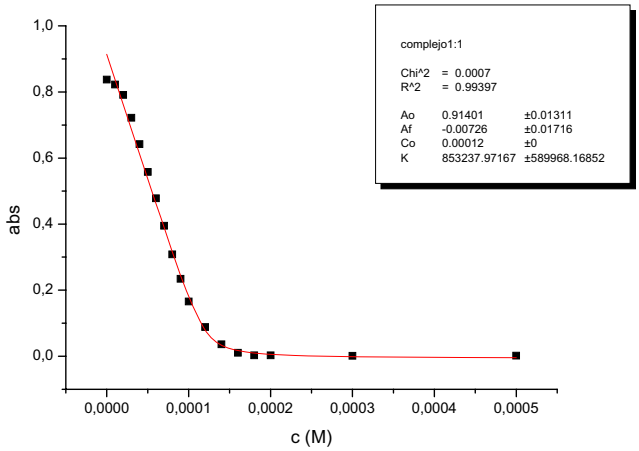

Fig. 40. Titration profile of **4** (10^{-4} M, CH_3CN) with Cu^{2+}

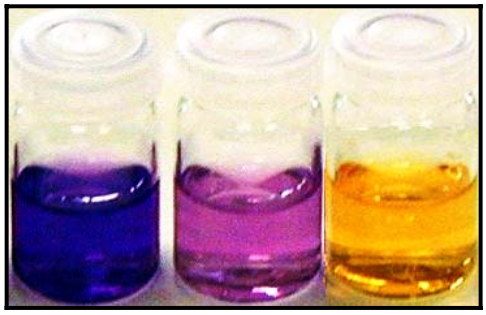

Fig. 41. Color changes of receptor **9** upon addition of 1 eq. of the cations. From left to right: none, Hg^{2+}, Cu^{2+}.

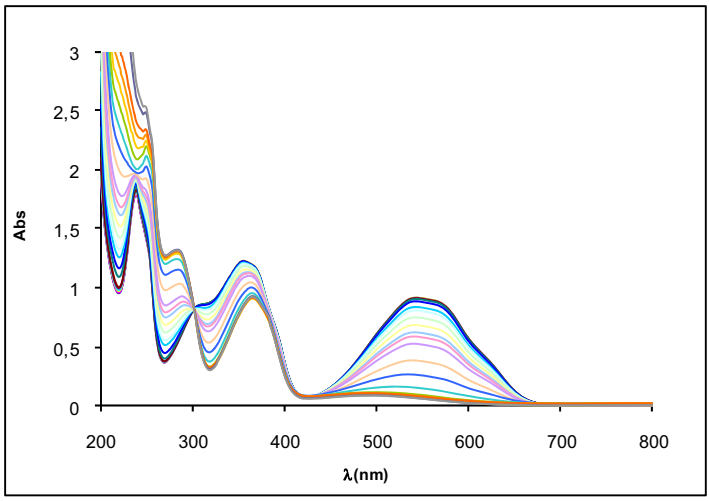

Fig. 42. UV titration of **9** (10^{-4} M, CH_3CN) with Hg^{2+}

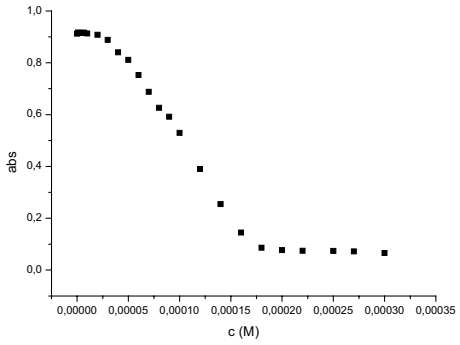

Fig. 43. Titration profile of **9** (10^{-4} M, CH_3CN) with Hg^{2+}

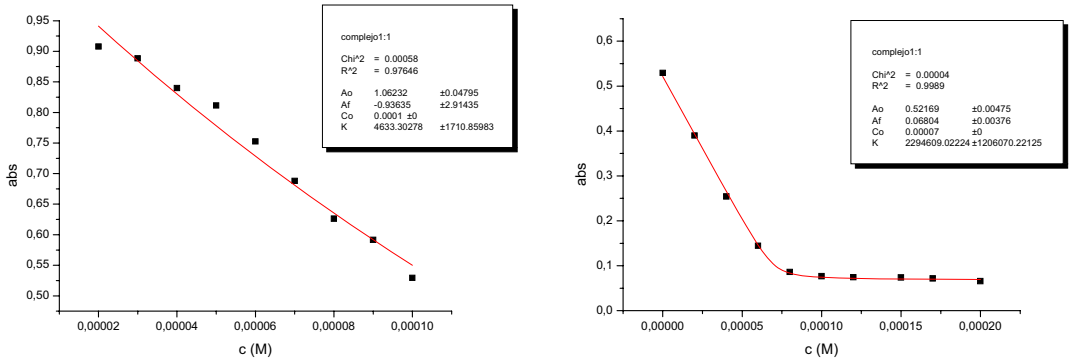

Fig. 44. Sequential fitting of the titration profile of **9** (10^{-4} M, CH_3CN) with Hg^{2+}

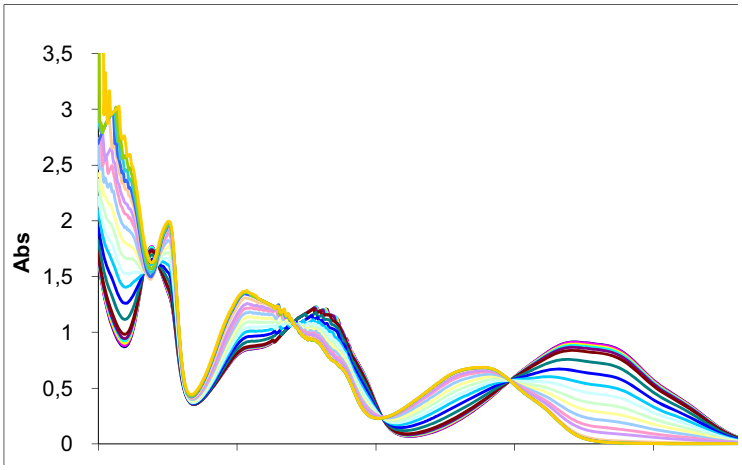

Fig. 45. UV titration of **9** (10^{-4} M, CH_3CN) with Cu^{2+}

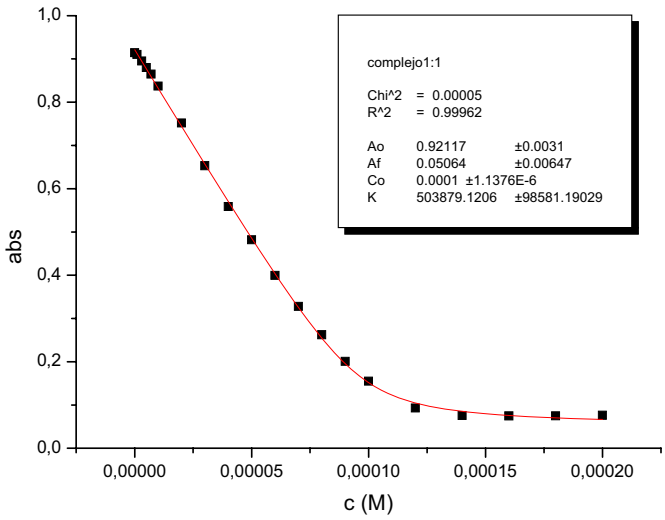

Fig. 46. Titration profile of **9** (10^{-4} M, CH_3CN) with Cu^{2+}

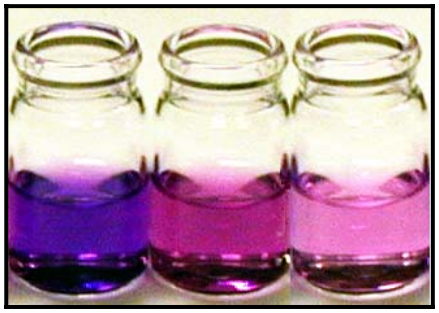

Fig. 47. Color changes of receptor **8** upon addition of 1 eq. of different cations. From left to right: none, Fe^{3+}, Pb^{2+}.

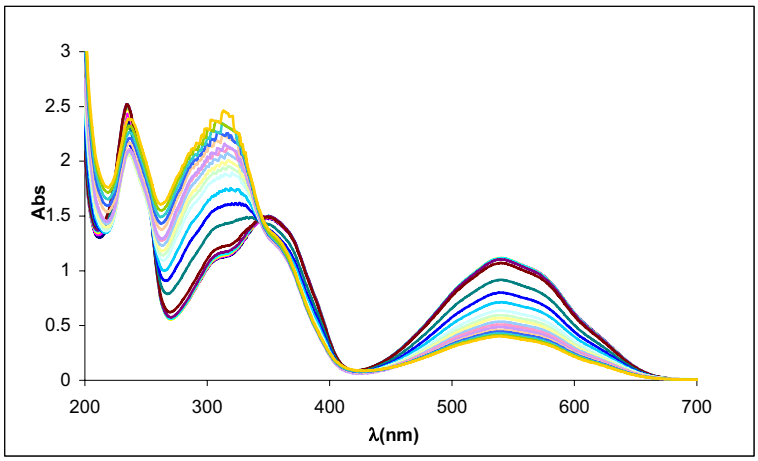

Fig. 48. UV titration of **8** (10^{-4} M, CH_3CN) with Fe^{3+}

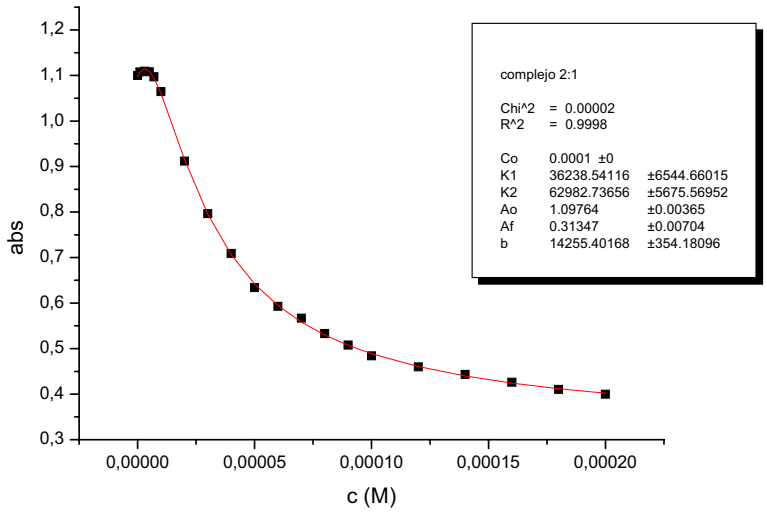

Fig. 49. Titration profile of **8** (10^{-4} M, CH_3CN/) with Fe^{3+}

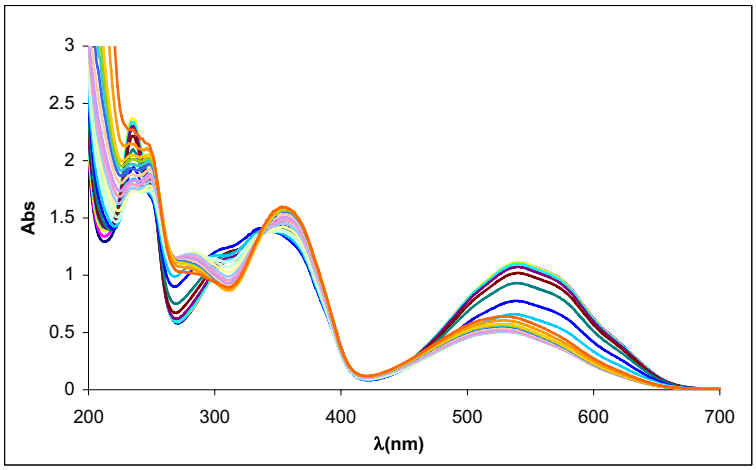

Fig. 50. UV titration of **8** (10^{-4} M, CH_3CN) with Pb^{2+}

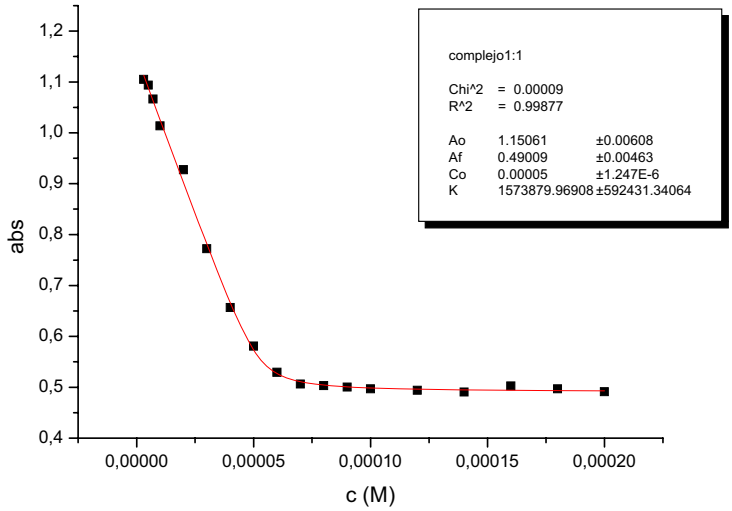

Fig. 51. Titration profile of **8** (10^{-4} M, CH_3CN) with Pb^{2+}

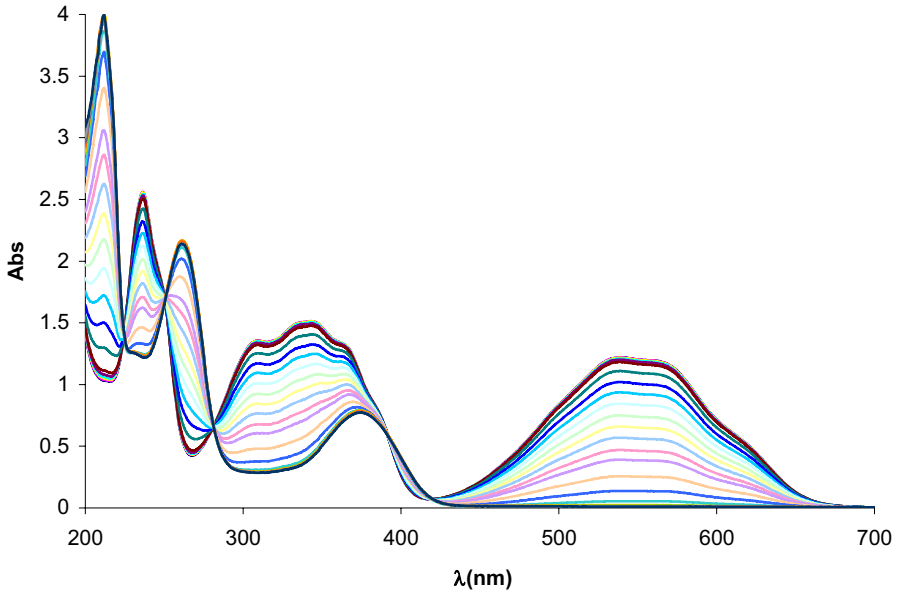

Fig. 52. UV titration of **2** (10^{-4} M, CH_3CN) with CN^-

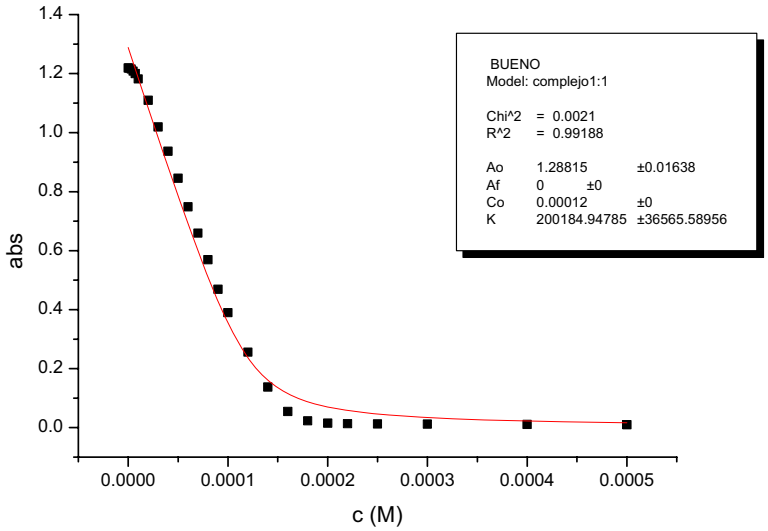

Fig. 53. Titration profile of **2** (10^{-4} M, CH_3CN) with CN^-

Fig. 54. Colour changes induced by the addition of 10 eq of different anions to a solution of receptor **4** (10^{-4} M in acetonitrile). From left to right: none, F^-, Cl^-, Br^-, I^-, BzO^-, NO_3^-, $H_2PO_4^-$, HSO_4^-, AcO^-, CN^-, SCN^-.

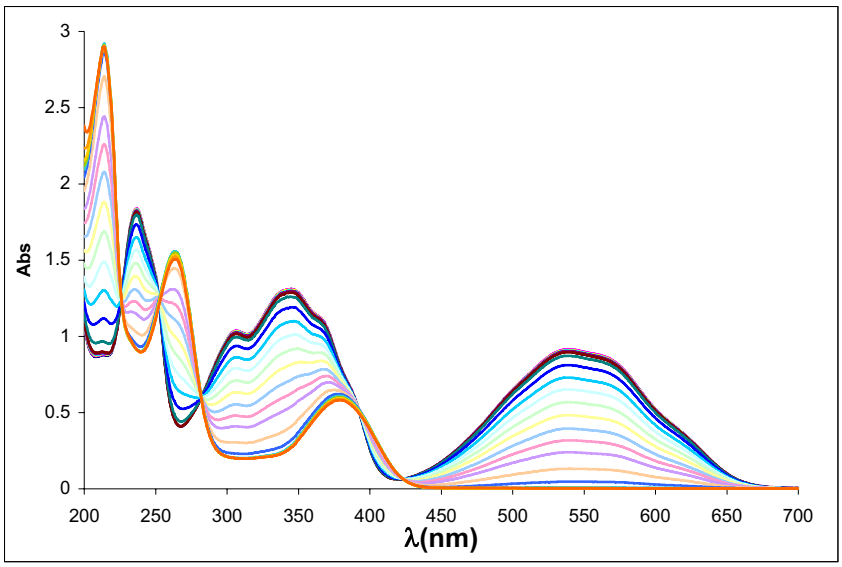

Fig. 55. UV titration of **4** (10^{-4} M, CH_3CN) with CN^-

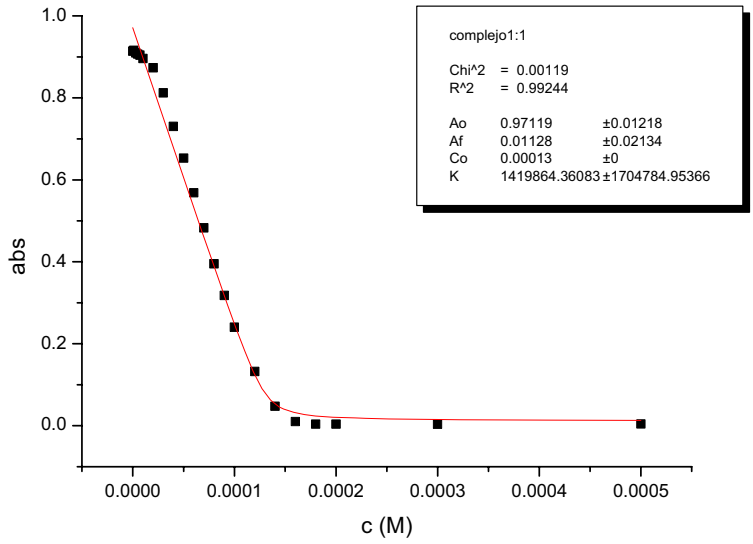

Fig. 56. Titration profile of **4** (10^{-4} M, CH_3CN) with CN^-

Job's plot analysis of 4 and 9 (10^{-4} M in MeCN) with Cu^{2+} and Hg^{2+}

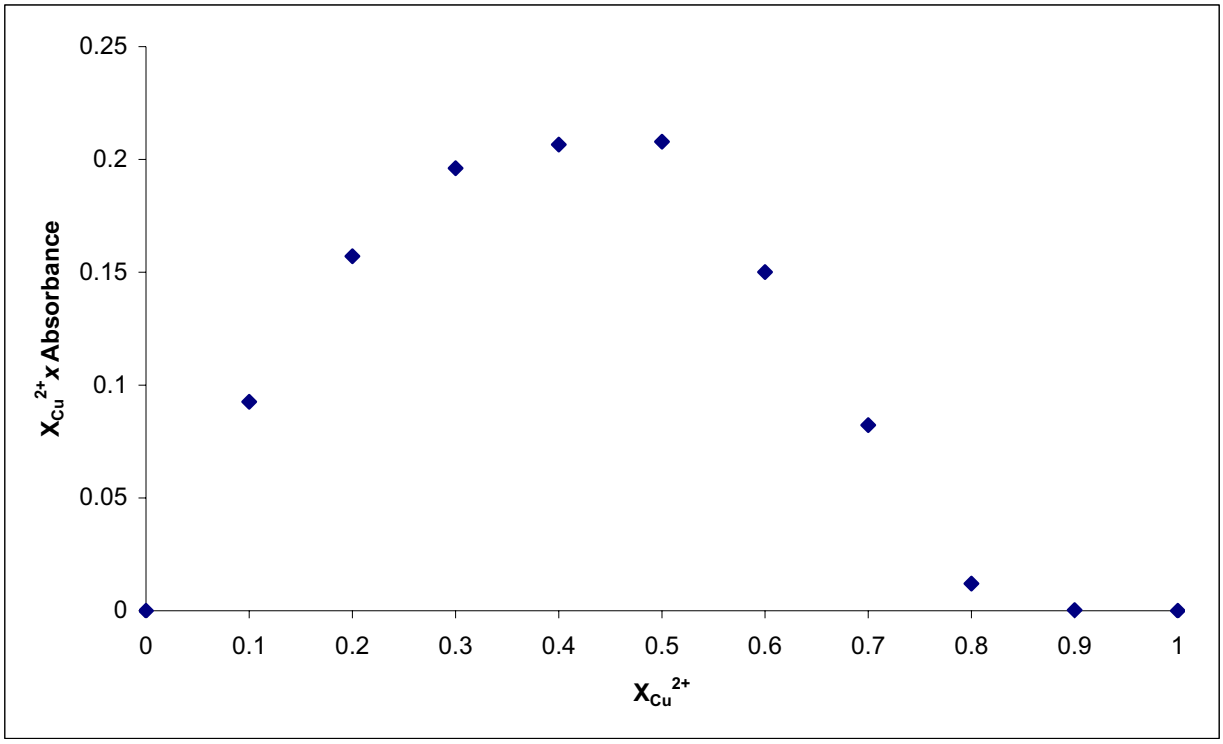

Fig. 57. Job plot analysis of **4** (10^{-4} M in MeCN) with Cu^{2+}

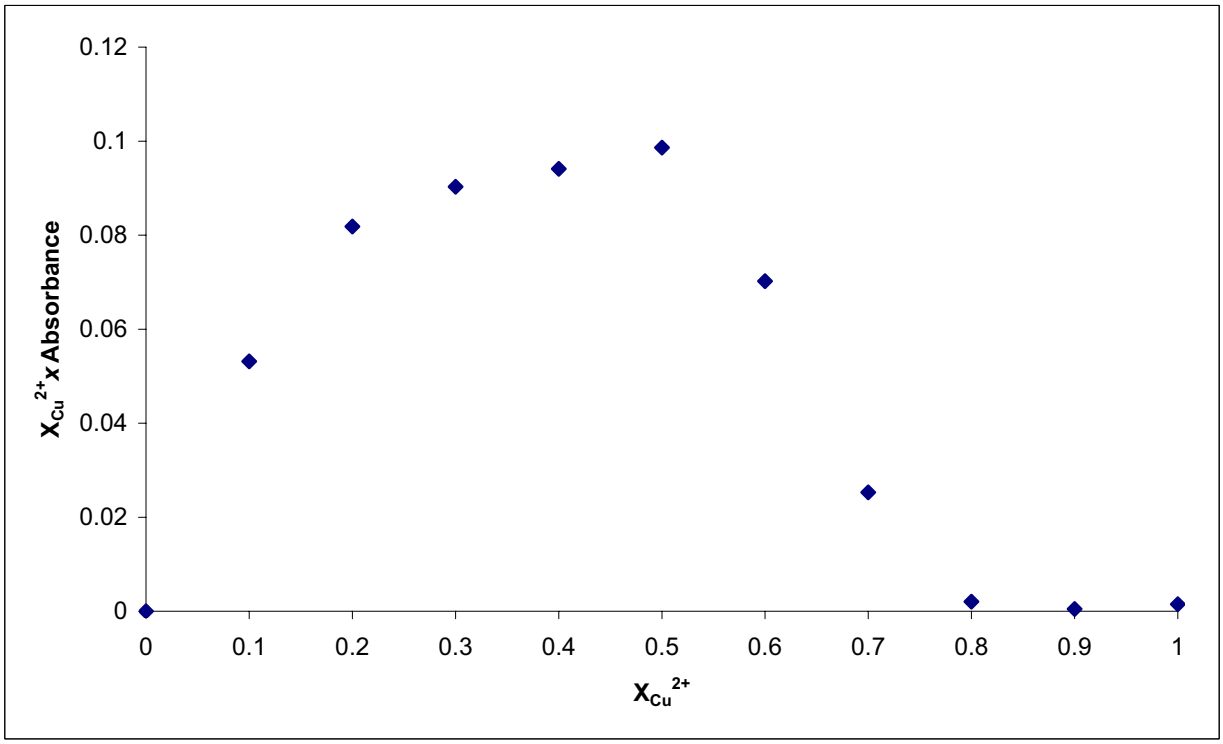

Fig. 58. Job's plot analysis of **9** (10^{-4} M in MeCN) with Cu^{2+}

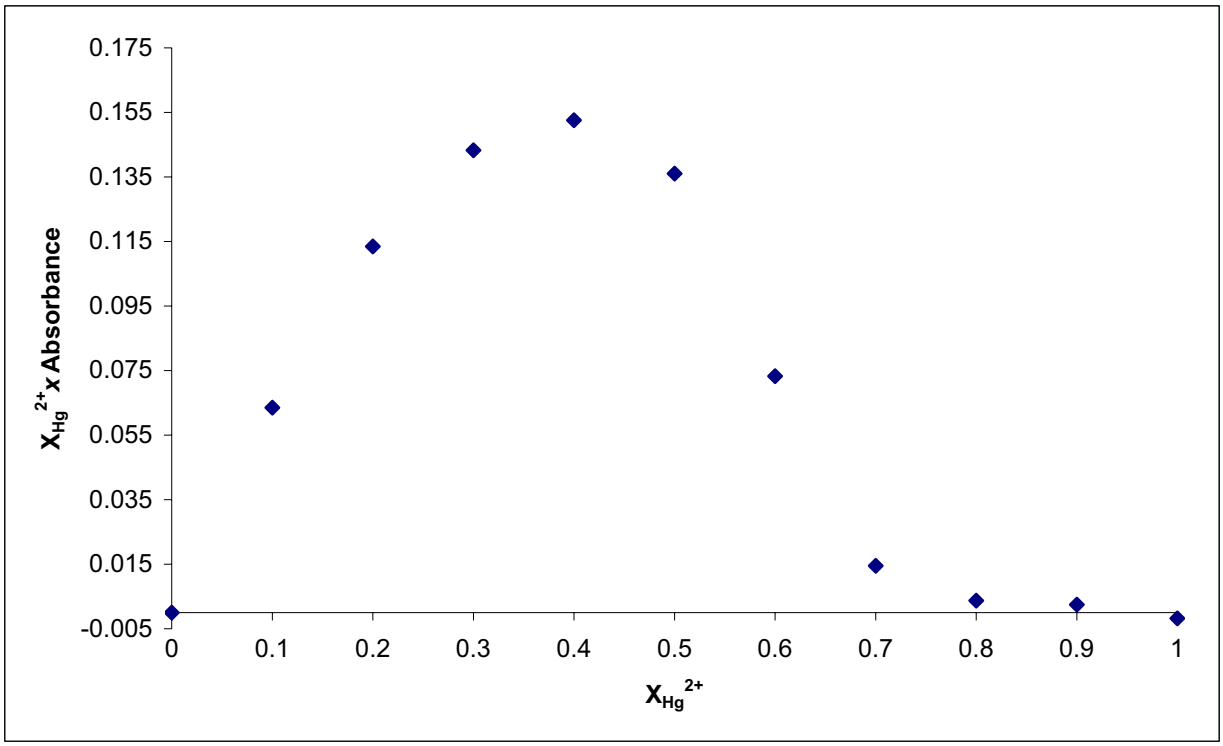

Fig. 59. Job's plot analysis of **9** (10^{-4} M in MeCN) with Hg^{2+}

5. Reversibility studies:

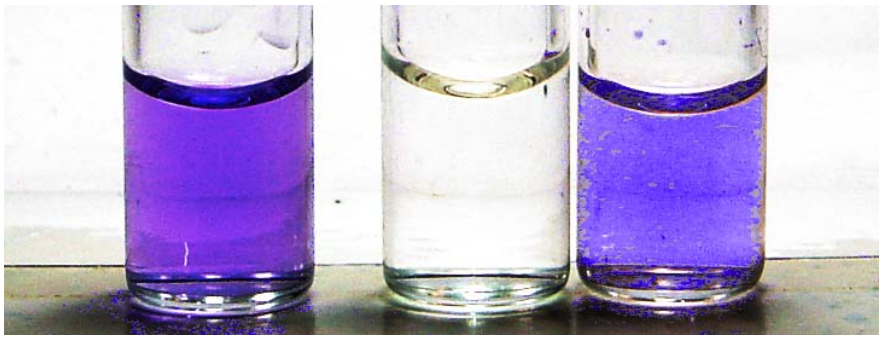

(a) (b) (c)

Fig. 60. (a) A solution of **4** (10^{-4} M in MeCN). (b) Addition of 4 eq of Cu^{2+} $(ClO_4^-)_2$ to solution (a). (c) Addition of 2 equiv of 3,6-dioxa-1,8-octanedithiole to solution (b).

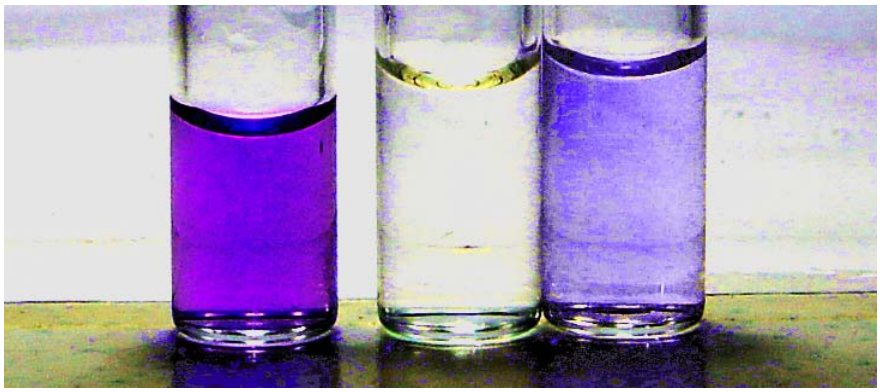

(a) (b) (c)

Fig. 61. (a) A solution of **2** (10^{-4} M in MeCN). (b) Addition of 4 eq of CN^- Bu_4N^+ to solution (a). (c) Addition of 4 equiv of Ag^+ ClO_4^- to solution (b).

MS titration experiments.

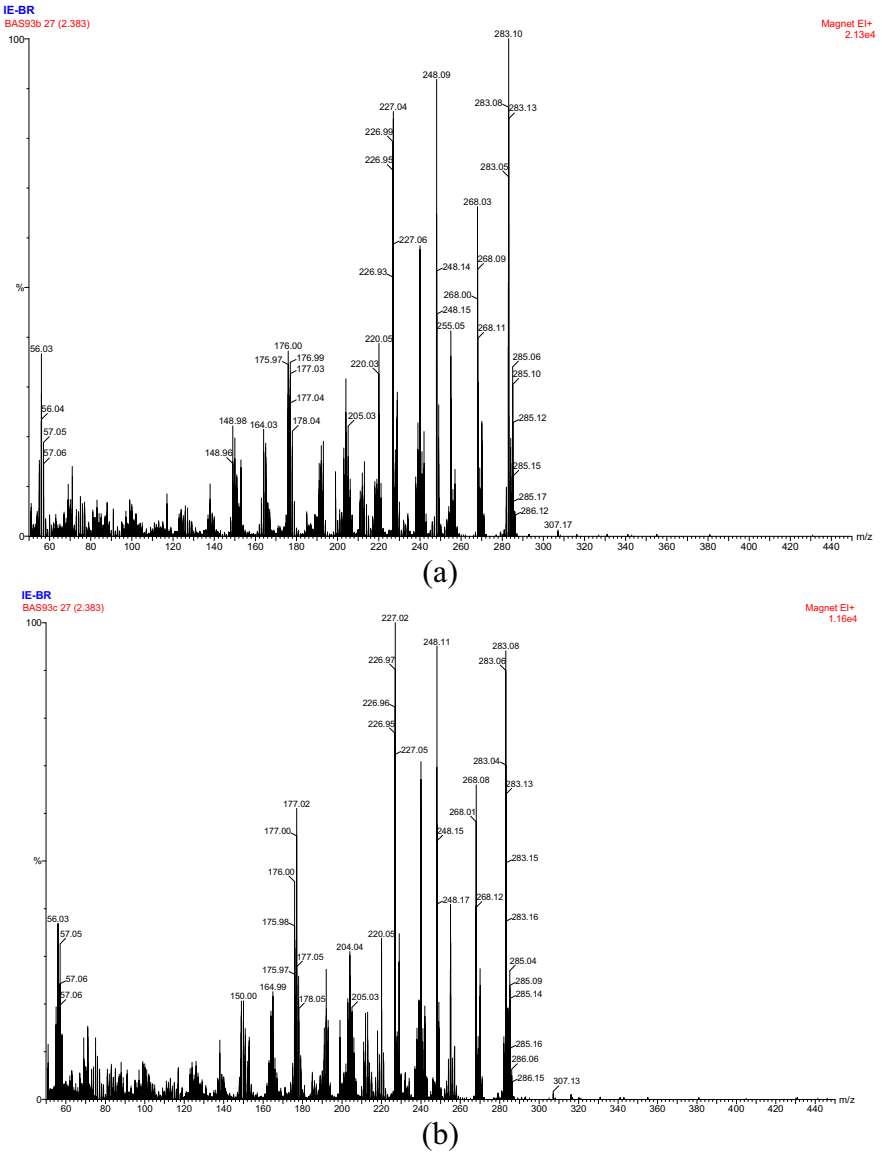

Fig. 62. (a) EIMS spectrum of **2**. (b) EIMS spectrum of **2** + 2 equiv CN^-

6. ^{1}H NMR titration studies

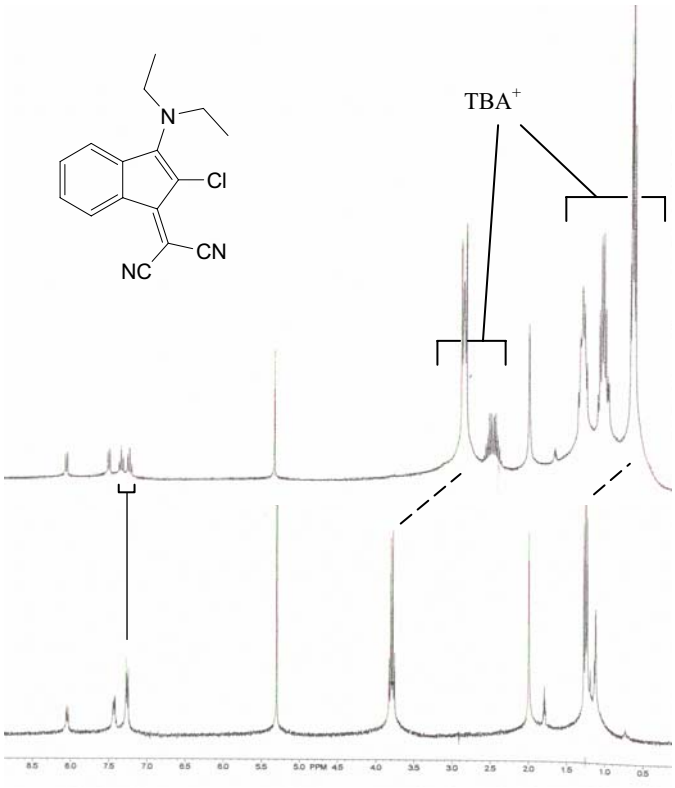

Fig. 63. Changes induced in the ^{1}H NMR spectra of **2** (200 MHz, 23 mM, CD_3CN, 20ºC) upon addition of 1 eq of TBACN.

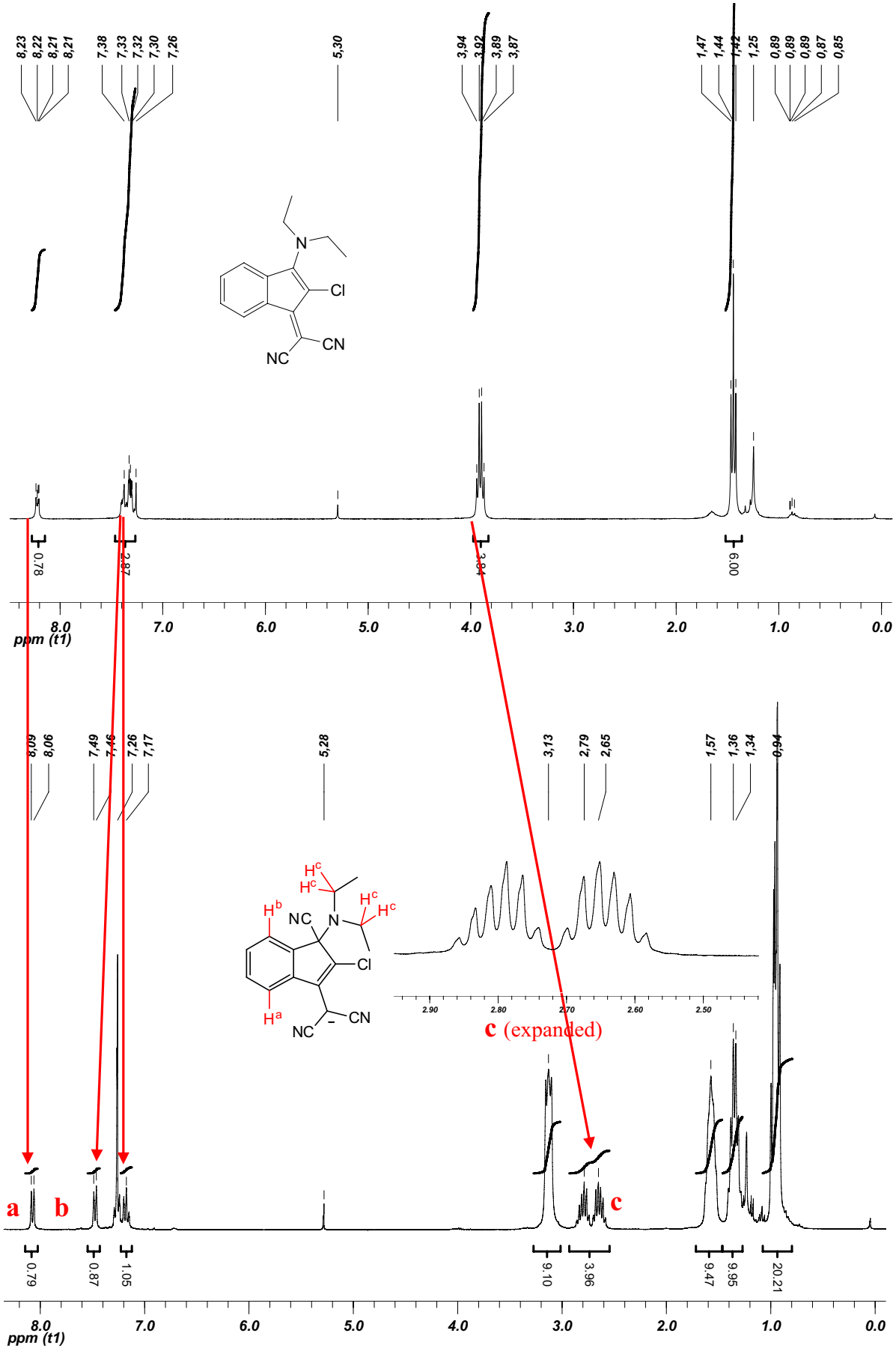

Fig. 64. A detailed comparison between ^{1}H NMR spectra of **2** before and after addition of 1 equiv CN^- ($CDCl_3$, 300 MHz)

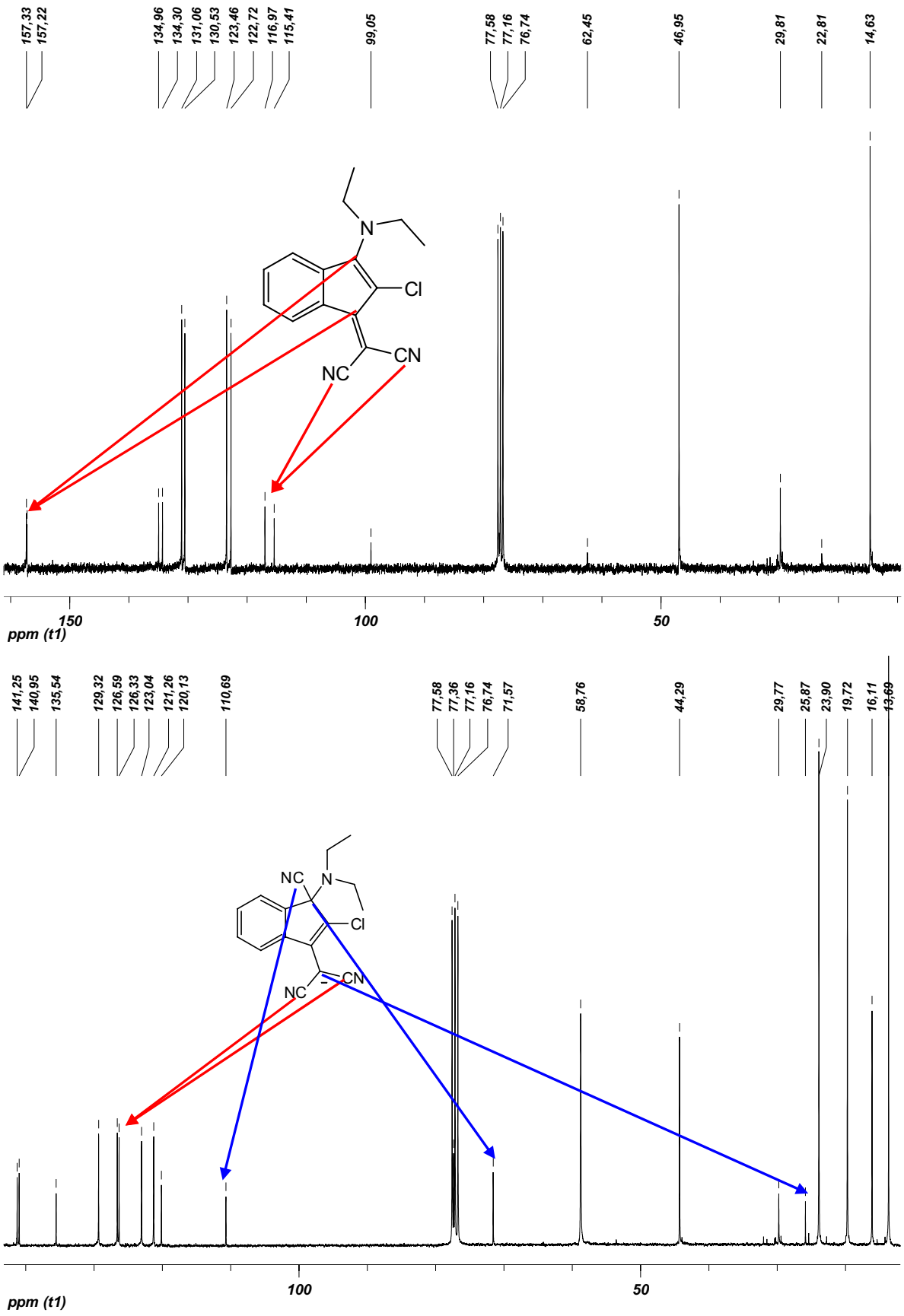

Fig. 65. A detailed comparison between ^{13}C NMR spectra of **2** before and after addition of 1 equiv CN^- ($CDCl_3$, 75 MHz)

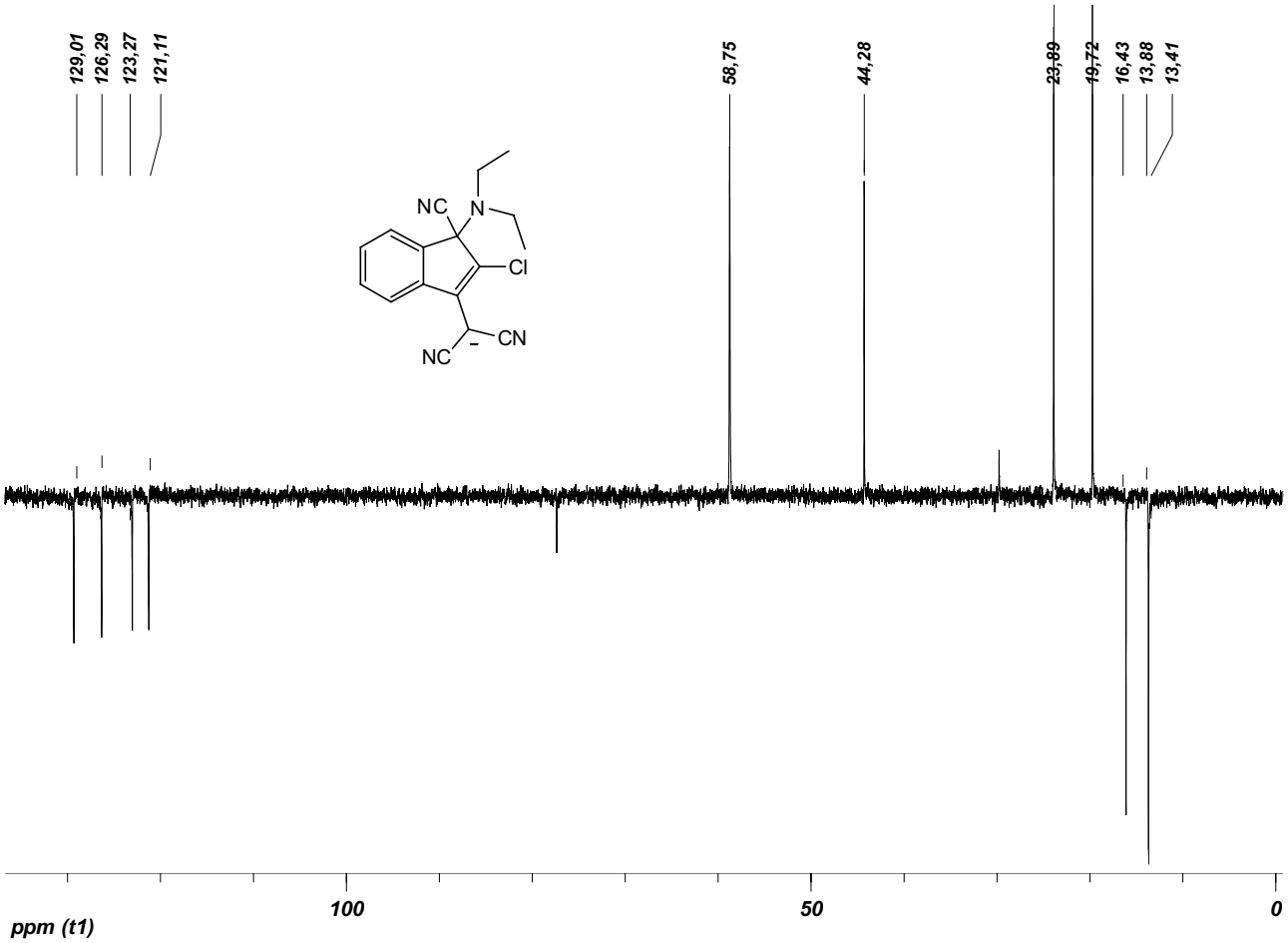

Fig. 66. DEPT experiment spectrum of **2** after addition of 1 equiv CN^- ($CDCl_3$, 75 MHz)

7. Kinetic studies: First order kinetics of reaction of 2 and CN^-

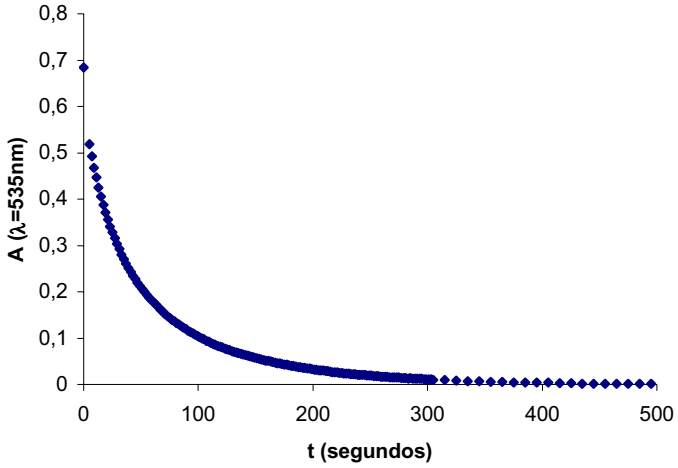

Fig. 67. Plot of evolution of absorbance and time of a mixture of **2** and CN^- (1:1), 10^{-4}M in CH_3CN

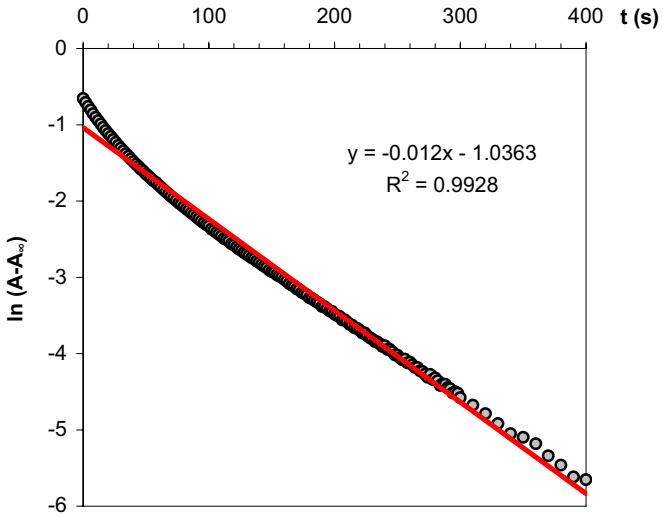

Fig. 68. Plot of a first order kinetics of $\ln(A-A_\infty)$ and t(s) of a mixture of **2** and CN^- (1:1), 10^{-4}M in CH_3CN that afforded the constant: $K_v=0.012s^{-1}$